Atmos. Chem. Phys., 23, 981–998, 2023
https://doi.org/10.5194/acp-23-981-2023

Atmospheric Chemistry and Physics
Open Access
EGU

African smoke particles act as cloud condensation nuclei in the wintertime tropical North Atlantic boundary layer over Barbados

Haley M. Royer[1], Mira L. Pöhlker[2,3,4], Ovid Krüger[2], Edmund Blades[5,6], Peter Sealy[5], Nurun Nahar Lata[7], Zezhen Cheng[7], Swarup China[7], Andrew P. Ault[8], Patricia K. Quinn[9], Paquita Zuidema[1], Christopher Pöhlker[2], Ulrich Pöschl[2], Meinrat Andreae[2,10,11], and Cassandra J. Gaston[1]

[1]Department of Atmospheric Sciences, Rosenstiel School of Marine, Atmospheric, and Earth Science, University of Miami, Miami, FL, USA
[2]Department of Multiphase Chemistry, Max Planck Institute for Chemistry, Mainz, Germany
[3]Leipzig Institute for Meteorology, Leipzig University, Leipzig, Germany
[4]Experimental Aerosol and Cloud Microphysics Department, Leibniz Institute for Tropospheric Research, Leipzig, Germany
[5]Barbados Atmospheric Chemistry Observatory, Ragged Point, Barbados
[6]Queen Elizabeth Hospital Barbados, Bridgetown, Barbados
[7]Environmental Molecular Sciences Laboratory, Pacific Northwest National Laboratory, Richland, WA, USA
[8]Department of Chemistry, University of Michigan, Ann Arbor, MI, USA
[9]Pacific Marine Environmental Laboratory, National Oceanic and Atmospheric Administration, Seattle, WA, USA
[10]Department of Geology and Geophysics, King Saud University, Riyadh, Saudi Arabia
[11]Scripps Institution of Oceanography, University of California San Diego, La Jolla, CA, USA

Correspondence: Mira L. Pöhlker (poehlker@tropos.de) and Cassandra J. Gaston (cgaston@miami.edu)

Received: 12 May 2022 – Discussion started: 24 May 2022
Revised: 7 October 2022 – Accepted: 8 November 2022 – Published: 20 January 2023

Abstract. The number concentration and properties of aerosol particles serving as cloud condensation nuclei (CCN) are important for understanding cloud properties, including in the tropical Atlantic marine boundary layer (MBL), where marine cumulus clouds reflect incoming solar radiation and obscure the low-albedo ocean surface. Studies linking aerosol source, composition, and water uptake properties in this region have been conducted primarily during the summertime dust transport season, despite the region receiving a variety of aerosol particle types throughout the year. In this study, we compare size-resolved aerosol chemical composition data to the hygroscopicity parameter κ derived from size-resolved CCN measurements made during the Elucidating the Role of Clouds–Circulation Coupling in Climate (EUREC^{4}A) and Atlantic Tradewind Ocean-Atmosphere Mesoscale Interaction Campaign (ATOMIC) campaigns from January to February 2020. We observed unexpected periods of wintertime long-range transport of African smoke and dust to Barbados. During these periods, the accumulation-mode aerosol particle and CCN number concentrations as well as the proportions of dust and smoke particles increased, whereas the average κ slightly decreased ($\kappa = 0.46 \pm 0.10$) from marine background conditions ($\kappa = 0.52 \pm 0.09$) when the submicron particles were mostly composed of marine organics and sulfate. Size-resolved chemical analysis shows that smoke particles were the major contributor to the accumulation mode during long-range transport events, indicating that smoke is mainly responsible for the observed increase in CCN number concentrations. Earlier studies conducted at Barbados have mostly focused on the role of dust on CCN, but our results show that aerosol hygroscopicity and CCN number concentrations during wintertime long-range transport

events over the tropical North Atlantic are also affected by African smoke. Our findings highlight the importance of African smoke for atmospheric processes and cloud formation over the Caribbean.

1 Introduction

Aerosol particle number, size, hygroscopicity, and chemical mixing state determine cloud droplet formation and, thus, fundamentally affect the radiative properties and lifetime of clouds (Twomey, 1977; Albrecht, 1989; McFiggans et al., 2006; Quinn et al., 2008; Zuidema et al., 2008). Quantifying the effect of aerosols on cloud radiative forcing, however, is still the single largest source of uncertainty in predicting temperature increases associated with climate change (Forster et al., 2021). This uncertainty is especially important to resolve in marine regions where aerosol–cloud interactions are understudied, even though the majority of Earth's surface is covered by oceans (Carslaw et al., 2013). The existing literature that explores marine aerosol–cloud interactions does so primarily at the mid to high latitudes of the North Atlantic, with few studies focusing on tropical latitudes where shallow cumulus clouds form (Behrenfeld et al., 2019; Sorooshian et al., 2020; Allan et al., 2008; Klingebiel et al., 2019; Rauber et al., 2007). Shallow cumulus clouds are important for Earth's climate as they are one of the most geographically pervasive cloud types and can influence Earth's radiative budget by reflecting incoming radiation over the low-albedo ocean surface.

Aerosol research conducted in the tropical Atlantic has focused largely on the long-range transport of mineral dust from northern Africa in the summertime. Long-range African dust transport occurs when emitted desert dust is lofted above the marine boundary layer (MBL) into the Saharan Air Layer (SAL) and is propagated westward (Carlson and Prospero, 1972). As dust is transported westward, it can mix into the underlying moist MBL and deposit into the Atlantic Ocean and Caribbean Sea as well as western Atlantic land masses such as South America, the Caribbean islands, and North America (Carlson and Prospero, 1972; Barkley et al., 2019; Prospero et al., 2020, 1981). Some studies have attempted to understand the effects of long-range transported dust on cloud droplet formation and water uptake, with varying results depending on the degree of aging that dust experiences during transport (Rosenfeld et al., 2001; Allan et al., 2008; Denjean et al., 2015; Wex et al., 2016; Kristensen et al., 2016). However, these studies provide conflicting results on whether dust particles are hygroscopic and numerous enough to appreciably impact cloud condensation nuclei (CCN) concentrations in the tropical Atlantic. Due to the annual oscillation of the intertropical convergence zone (ITCZ), dust transport also exhibits a seasonality in terms of its geographic extent (Adams et al., 2012; Chin et al., 2014; Prospero and Lamb, 2003; Prospero, 1968; Prospero and Mayol-Bracero, 2013; Yu et al., 2019; Zuidema et al., 2019). However, marine shallow cumulus clouds form year-round in the tropical Atlantic regardless of dust transport. Thus, it is important to focus on aerosol characteristics across a full seasonal cycle to obtain a thorough understanding of the role aerosols play in cloud formation in the tropical Atlantic (McCoy et al., 2022).

Few studies have attempted to fully understand which aerosols are the most prominent CCN during both the boreal summer (when dust concentrations are at a maximum) and the boreal winter (when dust concentrations are at a minimum) in the tropical North Atlantic MBL. African smoke is one particle type that may be important for CCN activation in the tropical North Atlantic but has been understudied at dust receptor sites like Barbados (Wex et al., 2016). In contrast to dust, previous research has shown that smoke particles are an important source of CCN (Pierce et al., 2007; Spracklen et al., 2011; Lathem et al., 2013; Edwards et al., 2021), with some research showing that smoke particles can activate at supersaturations as low as 0.05 % (Rogers et al., 1991).

There are a number of reasons that explain why smoke particles can be effective CCN. Smoke particles are often complex mixtures of both organic and inorganic components that change compositionally and morphologically during their residence time in the atmosphere (Reid et al., 2005; Wu et al., 2021; Cappa et al., 2020; Konovalov et al., 2021; Hodshire et al., 2019). Smoke properties may also vary between fires, depending on fuel type and moisture, combustion phase, wind conditions, etc. (Reid et al., 2005; Miles et al., 1995; Andreae, 2019). In general, smoke particles are often found in the accumulation mode of the aerosol size distribution and primarily contain particulate organic matter, black carbon, and inorganic components including potassium chloride salts (Reid et al., 2005). Upon emission, smoke can undergo chemical processing through photochemical and heterogeneous reactions, including the loss of chloride and the acquisition of sulfate and nitrate, creating potassium sulfate compounds in smoke that are often used as tracers of aged smoke and that can affect the hygroscopicity of smoke particles (Capes et al., 2008; Hennigan et al., 2010, 2011; Reid et al., 2005; Zauscher et al., 2013). Chemical processing can also lead to morphological changes as the condensation of gaseous compounds and multiphase processes with aqueous compounds can result in the growth and sphericity of smoke particles, which in turn can affect the CCN properties of smoke particles (Abel et al., 2003; Reid et al., 1998; Giordano et al., 2015; Zhang et al., 2008). The variations in the chemical and physical properties of emitted smoke particles as well as the changes these properties can undergo in transit

make it difficult to predict the ability of smoke particles to act as CCN.

In this study, we investigated the relationship between submicron aerosol composition and CCN in the tropical North Atlantic MBL under marine background conditions and conditions affected by long-range continental aerosol transport of smoke and dust particles (henceforth referred to as continental aerosol transport – CAT – conditions). To perform this work, we collected aerosol samples and size-resolved CCN data from January to February 2020 at the Barbados Atmospheric Chemistry Observatory (BACO) during the Elucidating the Role of Clouds–Circulation Coupling in Climate/Atlantic Tradewind Ocean-Atmosphere Mesoscale Interaction Campaign (EUREC^{4}A/ATOMIC) campaigns (Quinn et al., 2021; Stevens et al., 2021). Conducting this research during the boreal winter provided a unique opportunity to explore aerosol–cloud interactions under meteorological conditions different from those that are typically studied in the tropical North Atlantic. Dust primarily arrives in Barbados during the summer months, with peaks in June and July (Zuidema et al., 2019). As a result, dust receptor sites in Barbados have historically been used to compare CAT and marine background conditions during the boreal summer. During the winter, the southward shift of the ITCZ directs African dust to South America, resulting in a decrease in dust concentrations over Barbados during the winter months, with days in December and January sometimes receiving no dust at all (Prospero, 1968; Prospero et al., 2014; Prospero and Lamb, 2003; Prospero and Mayol-Bracero, 2013). However, during the EUREC^{4}A/ATOMIC campaigns, we observed anomalous wintertime transport of African aerosols to Barbados, which provided novel sampling conditions to study the effects of various aerosol types on cloud droplet formation. Specifically, we were able to explore how the addition of continental aerosols like mineral dust and smoke particles to background marine aerosols consisting of organics, sulfates, and sea salt affects CCN activity. This allowed us to compare the impact of ocean-derived vs. long-range transported aerosol on water uptake properties and CCN concentrations. We conclude this paper by discussing the importance of our findings for cloud formation in the tropical North Atlantic.

2 Methods

2.1 Measurement site and sampling period

Aerosol samples and size-resolved CCN data were collected at the BACO at Ragged Point during the EUREC^{4}A and ATOMIC field campaigns from 20 January to 20 February 2020 (Quinn et al., 2021; Stevens et al., 2021). Ragged Point (13°6′ N, 59°37′ W), a prominence on Barbados' eastern coast, is an ideal location for studying the impact of long-range African aerosol transport on aerosol–cloud interactions as it is situated on the most easterly island in the Caribbean and is exposed to the steady easterly trade winds. Thus, the eastern coast of the island is subject to little anthropogenic aerosol influence from local islands to the west (Prospero et al., 2005; Savoie et al., 2002). Further, the island is at a latitude coinciding with the outflow of African aerosols such as mineral dust (Prospero, 1968; Carlson and Prospero, 1972) and smoke particles (Archibald et al., 2015) as well as tropical marine cumulus clouds (Stevens et al., 2016).

2.2 Air mass origins

During the sampling period, air masses of varying compositions were observed at Ragged Point. To determine the origin of these air masses, 150 h back trajectories were generated every 6 h at heights of 500, 1000, and 1500 m throughout the campaign using the NOAA Hybrid Single-Particle Lagrangian Integrated Trajectory (HYSPLIT) model calculated using model vertical velocity and meteorology from the National Center for Environmental Prediction (NCEP) 1 ° Global Data Assimilation System (GDAS) (Stein et al., 2015; Rolph et al., 2017).

2.3 Dust concentration

To collect aerosols, the BACO is equipped with a high-volume sampler and an isokinetic aerosol inlet on top of a 17 m-tall tower situated on a 30 m bluff along the coast at Ragged Point. Daily dust mass concentrations were determined from filter-based measurements (Zuidema et al., 2019; Prospero et al., 2021) using a high-volume air sampler pumping at a rate of approximately 0.7 m^3 min^{-1} across a 20 cm × 25 cm cellulose Whatman-41 (W-41) filter with a nominal 20 µm pore size. W-41 filters were chosen for this analysis as they allow high flow rates and yield a collection efficiency of 95 % or better for dust (Kitto and Anderson, 1988) and submicron aerosols (Pszenny et al., 1993). Upper particle diameter limits for W-41 filters are approximately 80–100 µm or greater (Barkley et al., 2021). After aerosol collection, the filters are washed with Milli-Q water three times to remove soluble material and then placed in a furnace and combusted at 500 °C for about 12 h (i.e., overnight). Procedural blanks are also collected by placing a filter in the sampler for 15 min without turning on the pump. The resulting ash mass from a sample minus the mass of a filter blank is the gross ash weight, which is then adjusted by a factor of 1.3 to convert the ash weight to a mineral dust concentration. Previous research has confirmed the validity of this method for determining dust mass concentrations through chemical analysis of dust ash determined from filters collected in Barbados, crustal abundance, and soil dust composition (Zuidema et al., 2019). A correction factor of 1.3 is applied to the calculated dust concentrations to account for dust components such as bound water or soluble ions that are lost during the heating process (Zuidema et al., 2019; Prospero, 1999).

2.4 Aerosol chemical composition

Aerosol particles were sampled at ambient relative humidity (RH) through an isokinetic aerosol inlet and collected using a three-stage microanalysis particle sampler (MPS-3, California Measurements, Inc.), which samples particles from diameters of 5.0–2.5 µm (stage 1), 2.5–0.7 µm (stage 2), and < 0.7 µm (stage 3). For each set of samples (one set including one sample from each stage of the MPS), the MPS was run for 45 min at 2 L min^{-1} flow starting at approximately 09:30 LT (local time) or 13:30 coordinated universal time (UTC). Meteorological data from a local station were also used to manually check that wind direction fell between 335 and 130° and that wind speeds were greater than 1 m s^{-1} during all the sampling periods. Sampling under these wind conditions ensures that only air from the open ocean was sampled rather than local, anthropogenically influenced air.

To determine aerosol chemical composition, particles were deposited onto carbon-coated copper grids (Ted Pella, Inc.) that were later analyzed at the Pacific Northwest National Laboratory using computer-controlled scanning electron microscopy coupled with energy-dispersive X-ray spectroscopy (CCSEM/EDX; Quanta 3D) to determine the elemental composition of individual particles. We also collected samples on silicon wafers (Ted Pella, Inc.) which were analyzed with CCSEM/EDX to confirm the validity of the carbon measurements on the carbon-coated copper grids. Here, we focus only on the submicron particle population which exerts a greater influence on CCN number concentrations and is more sensitive to chemical changes that affect its hygroscopicity. Thus, for this study we focus primarily on data from stage 3 of the MPS, representing < 0.7 µm diameter particles.

CCSEM/EDX is a valid method for determining size-resolved chemistry of the aerosol loading as CCSEM excels in calculating particle size by imaging individual aerosols, while EDX provides the relative abundances for elements of interest (Tomlin et al., 2021). Percent composition threshold values of 1 % were used to ensure the presence of elements detected by the EDX. Single-particle analysis using CCSEM/EDX was limited to 16 elements found in common aerosols such as dust, sea salt, and smoke particles: carbon (C), nitrogen (N), oxygen (O), sodium (Na), magnesium (Mg), aluminum (Al), silicon (Si), phosphorus (P), sulfur (S), chlorine (Cl), potassium (K), calcium (Ca), vanadium (V), manganese (Mn), iron (Fe), and nickel (Ni). The EDX peak for Cu is heavily influenced by the background signal from the Cu grid and is excluded from analysis. Samples collected on Si substrates confirmed the validity of the C signal in analyzed particles, as the carbon coating on the Cu substrates has the potential to generate a background signal as well. An excess of 1000 particles was analyzed in each sample. Due to size limitations of the CCSEM, only particles with diameters > 0.1 µm were analyzed. Data products from CCSEM/EDX analysis were then analyzed in MATLAB (version 9.6.0; The Mathworks, Inc.) using a k-means clustering algorithm (Shen et al., 2016; Ault et al., 2012). The algorithm operates by generating categories of similar particles (clusters) based on the presence and intensity of elemental peaks in individual single-particle EDX spectra. These clusters are then assigned to particle types based on their size, morphology, characteristic EDX spectra, and the existing literature. A more thorough explanation of the k-means clustering algorithm and particle identification process includes the plots used to perform particle identification (Fig. S1 in the Supplement).

2.5 Size-resolved CCN measurements and data analysis

To determine the size-resolved CCN activity of aerosol particles during the sampling period, we used a continuous-flow streamwise thermal gradient CCN counter (CCNC, model CCN-100, DMT, Longmont, CO, USA; Roberts and Nenes, 2005; Rose et al., 2008) combined with a differential mobility analyzer (DMA, modified model M, Grimm Aerosol Technik, Ainring, Germany) and condensation particle counter (CPC, model 5412, Grimm Aerosol Technik). The method is described in detail in Pohlker et al. (2016). Flows for the size-resolved CCN setup included a sheath : sample flow ratio of 10 for the CCN counter (sample flow rate of 0.5 L min^{-1}), a sheath flow of 8 L min^{-1} for the DMA, and a sample flow of 0.6 L min^{-1} for the CPC. Upon entering the system, the sampled air was dried using a condensation drier to maintain a relative humidity (RH) between 20 % and 30 % and to ensure reliable hygroscopicity measurements. After drying, the particles passed through a DMA which selected particles with a diameter (D) between 20 and 245 nm. The monodisperse aerosol-laden flow was then split between the CCNC and CPC. Inside the CCNC, the particles were subjected to supersaturations (S) of 0.09 %, 0.16 %, 0.24 %, 0.43 %, and 0.74 %.

Calibrations of the CCNC supersaturations were performed according to the method described in Rose et al. (2008) by generating and size-selecting ammonium sulfate particles that were analyzed by the CCNC set to a designated temperature gradient as well as a CPC to measure total condensation nuclei (CN) values. Plots comparing CCN/CN and dry particle diameter were then used to determine the diameter at which 50 % of the particles in an aerosol population activate as CCN at a particular S, also called the critical activation diameter (d_{50}). D_{50} values were then used to determine supersaturation. Supersaturations were plotted against the designated temperature at the calculated supersaturation. The resulting plot provided a linear curve that could be used to adjust the supersaturation shown by the instrument to the actual value of the column supersaturation. After calibrating, S values averaged 0.08 %, 0.15 %, 0.23 %, 0.41 %, and 0.71 %.

For ambient sampling, particles that activate as CCN at each S and D are counted in the CCNC as CCN, while all particles of a selected D are counted in the CPC to determine the total aerosol concentrations of particles at each D. By scanning D at a given value of S, measurements from the CPC and CCNC are then used to generate an activation curve used to calculate the d_{50}. These values, along with the particle number size distribution determined by an SMPS (SMPS, Grimm model 5420 with CPC 3772) operating independently of the CCNC setup, are then used to calculate the effective hygroscopicity parameter κ using Eq. (1) according to the κ-Köhler model (Petters and Kreidenweis, 2007):

$$\kappa = \frac{4A^3}{27 D_p^3 \ln^2 S_{crit}}, \quad (1)$$

where D_p is the dry particle diameter, S_{crit} is the supersaturation set by the CCN counter, and A is the Kelvin term calculated from Eq. (2):

$$A = \frac{4\sigma M_w}{RT\rho_w}, \quad (2)$$

where σ is the surface tension ($\sigma = 0.072\ J\ m^{-2}$), R is the universal gas constant, M_w is the molecular weight of water, and ρ_w is the density of water. In the κ-Köhler model, higher values of κ indicate a more hygroscopic particle that is more efficient at taking up water and that can activate as CCN at lower S.

3 Results and discussion

In this section we will show that, upon arrival of co-transported dust and smoke, smoke originating from fires in the African Sahel dominates the accumulation-mode particle population in the tropical North Atlantic MBL, which results in an increase in CCN number concentration. Though dust and smoke are both transported to the region, smoke dominates the accumulation-mode number concentration by an order of magnitude compared to dust. These findings are supported by data products from dust mass concentrations, size-resolved hygroscopicity, single-particle data (CCSEM-EDX), and air mass history (NOAA'S HYSPLIT model), which all complement one another and provide unique insights into the aerosol sources, their single-particle composition, and their effects on cloud droplet activation.

3.1 Air mass characteristics during the EUREC^{4}A and ATOMIC campaigns

To confirm the origins of the various air masses sampled, we performed back-trajectory analysis throughout the campaign using NOAA's HYSPLIT model (Fig. 1) and quantified dust mass concentrations (Fig. 2a). Results of these two analyses show that Barbados was influenced by two types of air masses during the sampling period: air masses that, over the course of 6 d, do not pass over land (referred to as clean marine conditions) and air masses that have passed over the African continent (referred to as CAT events). Back-trajectory analysis was not conducted for time periods longer than 6 d, which introduces the possibility that marine air masses could have been influenced by European outflow as well. Figure 1 shows that during periods with low dust mass concentrations and a bimodal size distribution, air masses originated from the remote Atlantic Ocean at higher lati-

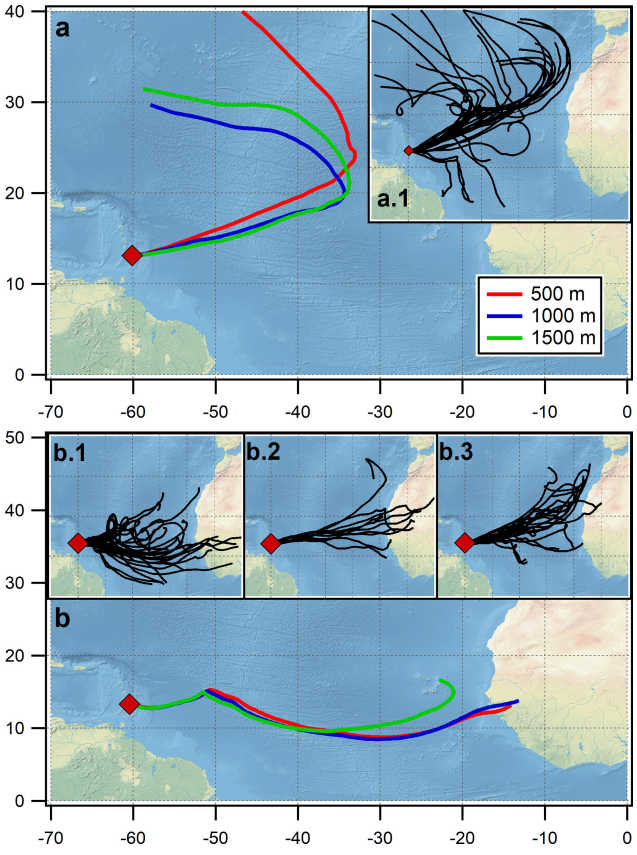

Figure 1. HYSPLIT back trajectories at Ragged Point, Barbados (red diamond), for the EUREC^{4}A/ATOMIC field campaign. **(a)** Back trajectories for 8 February 2020 18:00 UTC at heights of 500 m (red), 1000 m (blue), and 1500 m (green) exemplify air mass origins under clean marine sampling conditions. Subplot **(a.1)** shows all back trajectories from clean marine sampling conditions collected at 6 h intervals with a release altitude of 1000 m from 29 January 2020 00:00–29 January 2020 12:00, 6 February 2020 12:00–9 February 2020 18:00, and 12 February 2020 12:00–15 February 2020 06:00 UTC. **(b)** Back trajectories for 2 February 2020 18:00 UTC at 500, 1000, and 1500 m exemplify air mass origins under CAT conditions. The subplots **(b.1)**, **(b.2)**, and **(b.3)** show all back trajectories for three time periods during which continental aerosols were sampled: **(b.1)** 29 January 2020 18:00–6 February 2020 06:00, **(b.2)** 10 February 2020 00:00–12 February 2020 06:00, and **(b.3)** 15 February 2020 12:00–20 February 2020 18:00 UTC. Trajectories for **(b)** subplots were also collected at 6 h intervals with a release altitude of 1000 m.

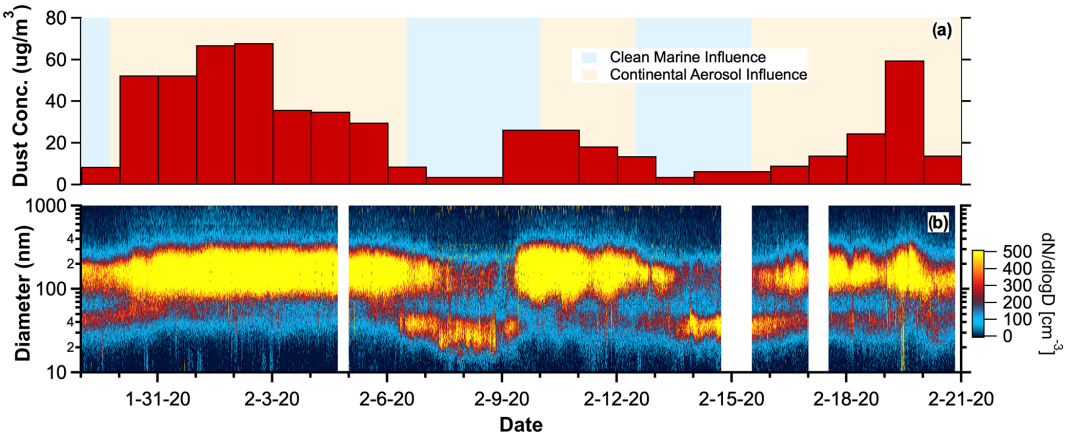

Figure 2. Temporal evolution of **(a)** dust mass concentrations determined from bulk aerosol filter samples and **(b)** submicron aerosol particle size distributions determined with an SMPS. Time for both plots is given in UTC (−4 h local Atlantic Standard Time). Color shading in panel **(a)** represents continental aerosol influence (orange shading) and clean marine influence (blue shading) **(b)** as determined by NOAA HYSPLIT back trajectories calculated at Ragged Point.

tudes with no land contact over 6 d. During time periods with high dust mass concentrations, air masses originated from continental Africa. Figure 2a shows that the total mass concentration of dust particles correlates very well with the arrival of air masses originating from Africa. During time periods when dust concentrations were low, the particle loading has a bimodal size distribution characteristic of clean marine air masses (Fig. 2b; Ault et al., 2013; Hoppel et al., 1986; O'Dowd et al., 2004). Upon the increase in dust mass concentrations, the submicron particle size distribution becomes unimodal and the smallest Aitken size mode is negligible, suggesting that long-range transported (LRT) particles are either dominant over the background marine particle loading or that smaller Aitken-mode particles are coagulating onto larger LRT continental aerosols to form a unimodal accumulation mode (Tomlin et al., 2021).

3.2 Single-particle aerosol composition

CCSEM/EDX analysis from the EUREC^{4}A and ATOMIC campaigns revealed the presence of several particle types with distinct chemistries and morphologies in the submicron aerosol loading (Ault et al., 2014; Behnke et al., 1997; Gaston et al., 2011a, 2013a). Figure 3 presents SEM images (left) and EDX spectra (right) for each particle type detected on stage 3 of the MPS (particle diameter < 0.7 µm), including sea spray, aged sea spray, mineral dust, internally mixed mineral dust and sea spray, sulfate, smoke, internally mixed mineral dust and smoke, and organics. Sea spray particles as well as internally mixed mineral dust and sea spray particles were dominant components of the supermicron aerosol loading but are only minor components of submicron aerosol.

3.2.1 Sea spray

Sea spray particles were characterized by high relative abundance of approximately equal parts Na and Cl, indicating the formation of halite (NaCl). Morphologically, sea spray particles have a cubic shape that represents the crystal structure of halite. Small Mg peaks approximately 10 % of the height of Na peaks were also observed in NaCl particles and reflect the Na : Mg ratio of seawater. Additional components of sea spray particles include rod-shaped particles containing Ca and S (presumably calcium sulfate) that were often found attached to NaCl particles (Ault et al., 2013; Bondy et al., 2018; Choël et al., 2007). Elements such as N and S that may suggest aging of sea spray were either absent or present in small relative abundance on NaCl components of sea spray particles.

3.2.2 Aged sea spray

Aged sea spray was defined by the presence of sea salt components including Na, Mg, K, S, and Cl. In contrast to freshly emitted sea spray particles, aged sea spray has a characteristically low or absent Cl signal with a strong presence of N or S. Figure 3 provides an example of an aged sea spray particle in which Na is high (indicating the presence of salt) but with a low Cl peak (suggesting the particle has been aged). The presence of S in this spectrum may explain the low relative abundance of Cl compared to Na. Sea spray can be aged through reactions with sulfuric acid (H_2SO_4), dinitrogen pentoxide (N_2O_5), and/or nitric acid (HNO_3), which results in Cl depletion and S or N enrichment (Gaston et al., 2011, 2013; Behnke et al., 1997; Ault et al., 2014, 2013a; Sobanska et al., 2003). Morphologically, aged sea salt particles had a similar appearance to fresh sea salt particles, which are often either cubic (as seen in Fig. 3) or appeared as a flaky

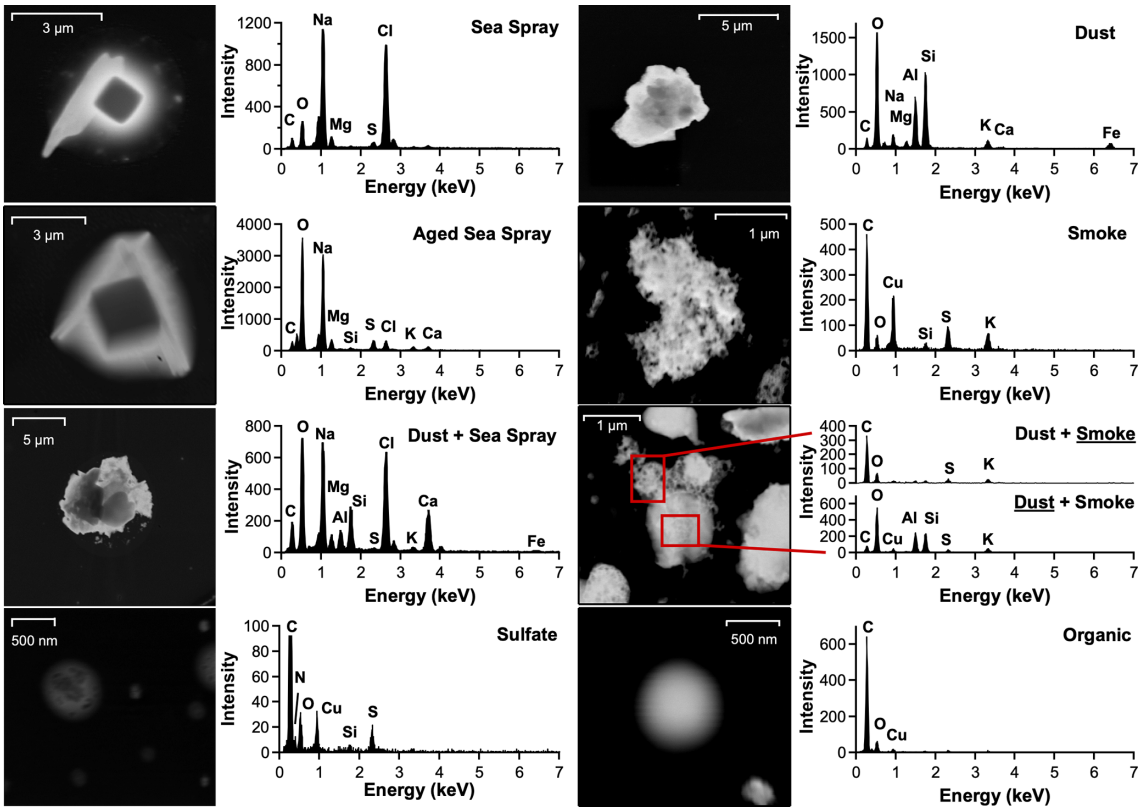

Figure 3. Characteristic aerosol particle types observed by SEM-EDX images (left) and spectra (right) in samples collected during the EUREC^{4}A/ATOMIC campaign. Spectra for the dust + smoke particle type represent different areas analyzed on the particle with EDX, denoted by the red boxes.

amorphous mass (Hoffman et al., 2004; Laskin et al., 2012; Li et al., 2010).

3.2.3 Mineral dust

Mineral dust is characterized by the presence of aluminosilicate elements such as Si, Al, Fe, K, Ca, and Mg in EDX spectra, which is consistent with previous studies of African dust (Twohy et al., 2009; Denjean et al., 2015; Hand et al., 2010; Levin et al., 2005; Krueger et al., 2004). Elements such as S and N were not observed in this particle type (Kandler et al., 2018), suggesting that detected dust had not undergone chemical processing during transport. Dust often appeared as a flaky or nodular amorphous mass as exhibited in Fig. 3 and the previous literature (Remoundaki et al., 2011; Laskin et al., 2005; Pachauri et al., 2013; Krueger et al., 2004).

3.2.4 Internally mixed mineral dust and sea spray

Particles containing elements indicative of both mineral dust (Si, Al, Fe, K, Ca, and Mg) and sea salt (approximately equal relative abundances of Na and Cl) were characterized as internally mixed mineral dust and sea spray (Choël et al., 2007; Deboudt et al., 2010; Sobanska et al., 2014). Elements such as S and N were often not present in this particle type, suggesting that the particles had not undergone atmospheric aging during transit. Particles containing both dust and sea spray components often appeared as conglomerates of multiple particles, with some parts containing more sea spray components and others containing more mineral dust components.

3.2.5 Sulfate

Sulfate-rich particles are a prevalent component of marine submicron aerosol (O'Dowd and de Leeuw, 2007) and characterized here by a dominant S component – often with high relative abundance of C, O, and N. These particles are likely sulfates bound to NH_4^+, such as ammonium sulfate $(NH_4)_2SO_4$ or ammonium bisulfate NH_4HSO_4 (Hand et al., 2010). The high relative abundance of C indicates a large organic fraction as well. The morphology of sulfate particles appeared smooth and spherical, as reported in the previous literature (Nájera and Horn, 2009).

3.2.6 Smoke

Smoke particles were identified by the presence of C with K and S likely representing internally mixed organic and black carbon with potassium-containing salts. K is a well-known indicator for biomass burning (Andreae, 1983; Li et al., 2003; Pósfai et al., 2003; Hudson et al., 2004; Murphy et al., 2006; Hand et al., 2010), especially under flaming conditions in savannah fires as opposed to smoldering conditions (Maenhaut et al., 1996; Echalar et al., 1995). Morphologically, smoke particles can be spherical due to aging or coatings but can also appear as aggregates or chains of spheroids (Hand et al., 2010; Pósfai et al., 2003; Miller et al., 2021; Dang et al., 2021). In this study, smoke particles most frequently appeared as small spherical particles.

3.2.7 Internally mixed mineral dust and smoke

Internally mixed mineral dust and smoke particles are characterized by dust components such as Si, Al, Fe, Ca, and Mg with strong contributions of K, S, C, and O. Morphologically, internal mixtures of dust and smoke appear as aggregates of amorphous dust particles with clusters or spheres representing soot from smoke. Single-particle chemical analyses of these particles show distinctions between the dust and smoke portions of the particles, with the dust portion having typical dust components (Si, Al, Fe, Ca, and Mg) and the smoke portion having typical smoke components (K and S with C and O). Previous research has observed internal mixing of carbonaceous particles and dust particles in Africa when significant amounts of both biomass burning and dust were present (Hand et al., 2010); however, we show that these internal mixtures can be transported all the way to the Caribbean as well.

3.2.8 Organics

Organic particles are defined by strong signals of C and O, with few other elements present, if any (Hand et al., 2010). The absence of S or N, which are often indicative of sulfate and nitrate, respectively, suggests that these particles have undergone minimal chemical aging. Morphologically, organic particles are characterized as small individual spheres. The organics were likely marine in origin (Russell et al., 2010) as they were the smallest particle type observed under both clean marine conditions and CAT conditions, which indicates that they may be a "background" aerosol type (Russell et al., 2010).

3.3 Arrival of anomalous wintertime co-transported dust and smoke

Figure 4 presents number fractions for particles detected in the submicron aerosol throughout the sampling period and reveals a similar trend in smoke particle number fractions to those of dust mass concentrations in Fig. 2, suggesting that smoke and dust were co-transported to Barbados from Africa. A similar plot to Fig. 4 that contains temporal chemistry from stage 1 and stage 2 of the MPS (representing supermicron particles of $> 0.7\,\mu m$ diameter) determined using CCSEM/EDX analysis can be found in the Supplement (Fig. S2). During the boreal winter, the Sahel region in northern Africa experiences its fire season in which large swathes of land are burned and large plumes of smoke are emitted from the region (Fig. S3; Ansmann et al., 2009; Barkley et al., 2019; Roberts et al., 2009). However, due to the southward shift in the ITCZ during boreal winter, smoke is expected to be transported primarily to South America (Moran-Zuloaga et al., 2018; Wang et al., 2016; Talbot et al., 1990). In our study, we observed the arrival of this smoke in Barbados. These findings are supported by temporal carbon monoxide (CO) column density measurements that are often used as a tracer for smoke (Figs. S4 and S5). Periods that correspond to clean marine influence are dominated by sulfate and organic particles in the submicron aerosol (Fig. 4). Upon arrival of continental aerosols, wildfire smoke appeared to dominate the number fraction of submicron aerosol.

Figure 5 presents size-resolved chemical data from CCSEM/EDX analysis from clean marine periods (average of all the clean marine periods) and one exemplary time period influenced by continental air masses (CAT event 1). Similar plots for other CAT events are provided in the Supplement (Fig. S6). Average particle diameters for each particle type detected during each sampling period are also provided in Table S1. Figure 5 shows that, in the clean marine periods, a small fraction of large particles have both a smoke and a dust signature. This suggests that our "clean marine conditions" are only "clean" relative to time periods dominated by dust and smoke rather than pristine clean marine conditions without any continental aerosol influence. The CAT event plot in Fig. 5 demonstrates that dust as well as internally mixed dust and smoke particles dominate in the submicron aerosol loading, followed by smoke. Smoke particles follow as the next-largest particle type. Organics dominate in the smallest size fractions, followed by sulfates, suggesting a secondary source for sulfate (Bates et al., 1992). Aged sea salt particles were on average smaller than most dust, internally mixed dust and smoke, and smoke particles. Figure 5 also shows that, at a diameter of $\sim 0.1\,\mu m$ (which is approximately the d_{50} of CCN at S 0.16 % under clean marine conditions and CAT conditions), the composition is dominated by sulfates and organics in the clean marine conditions, while smoke and organics dominate in the CAT event. The large decrease in sulfate number fraction during CAT events might be caused by the condensation of Aitken-mode sulfate-containing particles onto larger, long-range transported particles as indicated in Fig. 2 (Gaston et al., 2010).

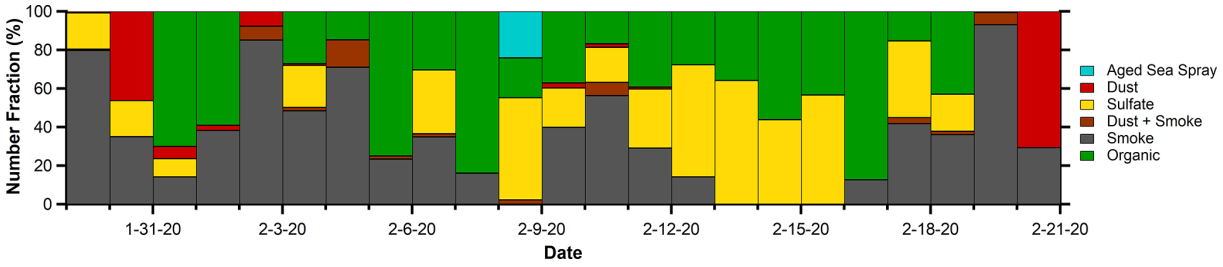

Figure 4. Temporal evolution of submicron number fractions for different types of aerosol particles determined by CCSEM/EDX analysis. The total number of particles analyzed for each day ranges from 1000 to 20 000.

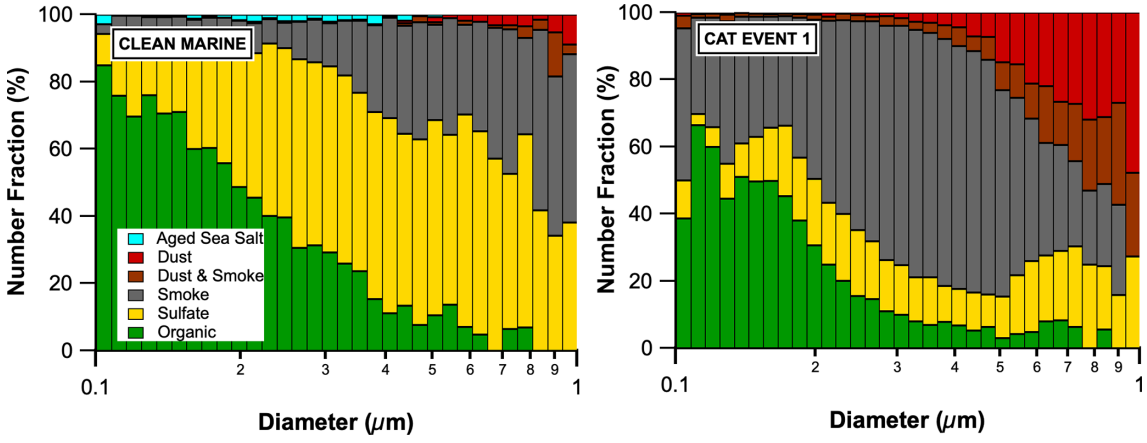

Figure 5. Number fractions of different types of submicron aerosol particles plotted against particle diameter. The "clean marine" plot (left) includes data from all clean marine sampling periods. The "CAT event 1" plot (right) includes data from the first period in which dust and wildfire smoke were observed over Barbados (29 January 2020 18:00–6 February 2020 06:00 UTC). Particles were organized into 32 size cuts (bins) to maximize the resolution of size-resolved chemical data. Particle counts in each bin range from 34 particles to 3041, with an average bin count of 493 particles for the clean marine plot and 973 for the CAT event plot.

3.4 Changes in aerosol hygroscopicity during EUREC^{4}A/ATOMIC

Comparisons between κ and submicron single-particle elemental composition reveal that smoke particles lower the hygroscopicity of the submicron aerosol compared to marine-derived submicron aerosol in the tropical North Atlantic. Figure 6 presents box plots for κ values as well as average d_{50} measured at each S under both clean marine conditions and CAT conditions. Both plots show a similar trend in which average κ increases from 0.09 % S to 0.24 % S. Then, with each subsequent increase in S after 0.24 % S, κ decreases as smaller, less hygroscopic particles activate at higher supersaturations. The low hygroscopicity of these smaller particles can be explained by compositional changes in the aerosol loading exhibited in Fig. 5, reflecting the shift in particle chemistry from mostly sulfate to mostly organic with decreasing particle size. Also of note is the κ of 0.6 observed for clean marine conditions at 0.24 % S, which matches κ measurements for ammonium sulfate particles that can dominate along with sea spray organics under clean marine conditions (Petters and Kreidenweis, 2007).

There is also a noticeable drop in average κ between the same supersaturations under clean marine conditions compared to CAT conditions. For example, at 0.16 % S, $\kappa = 0.52 \pm 0.09$ for all clean marine condition periods and $\kappa = 0.46 \pm 0.10$ for all continental aerosol transport periods. This is likely due to the addition of less hygroscopic material such as dust and smoke particles that are not dominant under clean marine conditions. As expected, trends in average d_{50} for both plots indicate that smaller particles activate as CCN with larger supersaturations. Activation diameters under CAT conditions are also larger than corresponding activation diameters under clean marine conditions for the same supersaturation. This also suggests that the addition of less-soluble material from transported smoke particles lowers the hygroscopicity and increases the activation diameter.

When comparing hygroscopicity data from this study to previous research, we find both similarities and differences in κ trends. For example, Good et al. (2010) present data collected in the tropical eastern Atlantic that provide an ideal comparison to our findings. On average, their values for κ under clean marine conditions and during observations of dust transport ($\kappa = 1.15$–1.4 and 0.8–0.92, respectively)

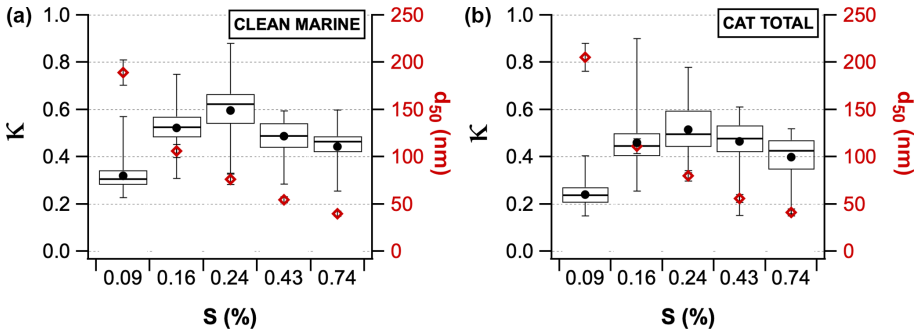

Figure 6. Hygroscopicity parameter κ (**a**; box plots) and corresponding mean diameter at which 50 % of the particles in an aerosol population activate as CCN at a particular S, also called the critical diameter "d_{50}" (**b**; red markers) for the investigated supersaturations (S). Whiskers on "d_{50}" markers represent standard deviation values of "d_{50}". Black dots in the box plot indicate κ mean values. Boxes represent the upper quartile, median, and lower quartile κ values at each S. Whiskers represent the upper and lower limits of κ at each S.

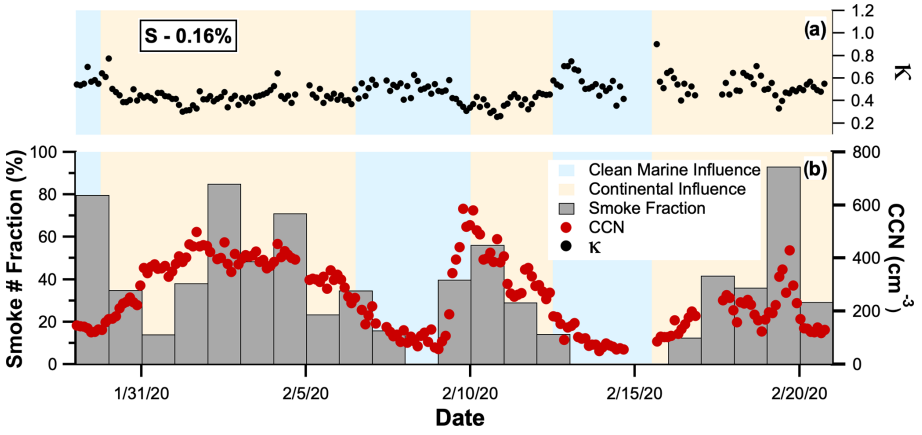

Figure 7. Temporal evolution of the hygroscopicity parameter κ (black dots, **a**) and CCN number concentration (red dots, **b**), both measured at $S = 0.16\,\%$, and smoke particle number fraction (grey bars, left axis, **b**). Background color shadings indicate periods of continental influence (orange) and clean marine influence (blue) determined by HYSPLIT back trajectories and dust mass concentrations.

were much higher than our observed values. However, Good et al. (2010) show similarities to our work through the distinct drop in κ between clean marine conditions and CAT conditions, which is attributed to the addition of hydrophobic dust to the aerosol loading. Wex et al. (2016) present CCN data from ground-based field sampling in November and April at Ragged Point, Barbados. They show a similar trend in κ in which values increase from 0.1 % S, peak at 0.2 % S, and then decrease with each subsequent increase in S. They also found a similar drop in κ upon the arrival of long-range transported aerosols, likely due to fewer hygroscopic particles from continental sources activating as CCN. A separate study from Kristensen et al. (2016) conducted similar research at Ragged Point, Barbados, during the boreal summer. The range in κ values of 0.2–0.5 matches that observed in our work, especially during CAT events. However, Kristensen et al. (2016) determined that concentrations of dust, sea salt, and soot were too small to influence CCN, concluding that sulfates and organics were the primary CCN types. They conclude that the low κ values observed during their sampling were due to organic compounds activating as CCN. We find similar κ values to Kristensen et al. (2016) and a similar particle chemistry of the accumulation and Aitken modes during clean marine conditions, suggesting that organics and sulfates were the primary CCN types under clean marine conditions studied for the EUREC^{4}A and ATOMIC campaigns as well. We also observe a drop in κ from clean marine conditions to CAT events. This drop in κ indicates the influence of an additional CCN particle type contributed by the CAT events.

3.5 African smoke particles enhance CCN concentrations

Comparisons between smoke fractions and CCN counts suggest that smoke particles enhance the number of CCN in the tropical North Atlantic MBL. Figure 7 presents two temporal plots of κ (Fig. 7a) and smoke number fractions with CCN counts measured at 0.16 % S (Fig. 7b). Table 1 provides averages of CCN concentrations for each time period shown in

Table 1. Values for average CCN concentrations and κ measured at 0.16 % S during each clean marine influence period and CAT event sampled during the EUREC^{4}A and ATOMIC campaigns.

Sampling period	Day/time (yyyy/mm/dd)	CCN concentrations (pt cm^{-3})	Average κ
Clean marine period 1	2020/01/29 00:00–2020/01/29 12:00	140 ± 10	0.58 ± 0.07
CAT event 1	2020/01/29 18:00–2020/02/06 06:00	340 ± 90	0.44 ± 0.08
Clean marine period 2	2020/02/06 12:00–2020/02/09 18:00	150 ± 98	0.50 ± 0.10
CAT event 2	2020/02/10 00:00–2020/02/12 06:00	400 ± 106	0.38 ± 0.06
Clean marine period 3	2020/02/12 12:00–2020/02/15 06:00	100 ± 42	0.55 ± 0.10
CAT event 3	2020/02/15 12:00–2020/02/20 18:00	190 ± 75	0.54 ± 0.10

Fig. 7b. Table S2 also provides average and median counts of analyzed smoke particles calculated for each CAT event, including CAT event 3, which had fewer smoke particles and a higher κ compared to other CAT events. Figure 7 suggests that there is an inverse relationship between κ and smoke number fractions in which an increase in smoke particles results in a decrease in κ. This is likely due to the activation of smoke particles as CCN, which are on average less hygroscopic than the sulfate particles that act as CCN under clean marine conditions. Figure 7b shows a positive correlation between smoke number fractions and CCN counts. A correlation plot of smoke number fraction and CCN concentrations is also provided in Fig. S7 to further emphasize their direct relationship.

There are multiple possible explanations for why African smoke particles may have acted as CCN. As shown in Fig. 5, smoke particles are larger than organics and sulfates, on average, and dominate sulfate and organic particle number concentrations upon arrival of long-range transported African aerosols. In this case, the relatively large size of the smoke particles makes for better CCN compared to organics or sulfates via the Kelvin effect (Dusek et al., 2006). The presence of salts in smoke particles has also been shown to be an important component in smoke hygroscopicity and may explain why smoke particles are efficient as CCN. Previous studies have shown that smoke particles often contain hygroscopic salts such as potassium chloride, potassium sulfate, and potassium nitrate (e.g., KCl, KNO_3, and K_2SO_4) (Freney et al., 2009; Zauscher et al., 2013; Dang et al., 2022). Other research also shows that only small fractions of salts are needed to increase aerosol hygroscopicity (Roberts et al., 2002). Based on CCSEM/EDX analysis, we find evidence that potassium sulfate salts may be present in transported smoke particles and thus may explain the potential for smoke to act as CCN.

4 Conclusions

Under clean marine conditions, the submicron aerosol loading consists primarily of sulfate and organic particles. CCN measurements determine cloud activation by particles approximately 80 nm in activation diameter with an average $\kappa = 0.52 \pm 0.08$ for 0.16 % S. Comparisons between particle size, hygroscopicity, and single-particle elemental composition suggest that sulfate particles (likely ammonium sulfate) are the primary CCN particles under clean marine conditions. During the EUREC^{4}A/ATOMIC campaigns, Barbados received three African aerosol transport events during which we detected mineral dust and smoke particles from northern Africa. Upon the arrival of African aerosols at the BACO, the CCN average activation diameter increased to approximately 200 nm, while the average hygroscopicity of activated particles for all CAT events decreased to $\kappa = 0.45 \pm 0.1$ for 0.16 % S. Upon arrival of high concentrations of smoke particles in Barbados, smoke particles dominate the accumulation-mode particle loading, decrease aerosol hygroscopicity, and also increase CCN number concentrations, which could also increase the cloud droplet number concentration and alter cloud radiative properties (Twomey, 1974). Overall, we find that smoke has a large effect on CCN number concentrations during the boreal winter, when smoke transport is high.

The observation of smoke transported to Barbados during the boreal winter also indicates the large geographic extent of African smoke that can impact the MBL. Building upon recent work from Ragged Point and other parts of the tropical and subtropical Atlantic (Schill et al., 2020; Kacarab et al., 2020; Zuidema et al., 2018; Holanda et al., 2020), this work also indicates a need for greater consideration of the impacts of smoke in the MBL, especially during the boreal winter. Previous research conducted at Ragged Point has primarily focused on African dust, which reaches its maximum during the boreal summer, when smoke transport is low (Zuidema et al., 2019). To better contextualize our findings, we analyzed carbon monoxide column density (a tracer for smoke) as well as aerosol optical depth (AOD; a tracer primarily for dust) from 2018 to 2022 (Figs. S4 and S5). Figure S4 shows the temporal trends, while Fig. S5 show seasonal averages. As expected, AOD peaks in July, when dust transport reaches a maximum. However, Figs. S4 and S5 indicate that smoke is decoupled from dust, reaching a maximum in the spring around April and a minimum in the

summer, when dust transport is highest. This finding suggests that, while the dust transport during the EUREC4A/ATOMIC campaigns is higher than average dust loadings during this month (Zuidema et al., 2019), the amount of smoke observed is not unique but rather characteristic of the region. This is consistent with observations in Amazonia, where smoke and dust transport during boreal winter and spring has been found consistently since the first measurement campaign in 1987 (Talbot et al., 1990; Andreae et al., 2015; Moran-Zuloaga et al., 2018). Further, wintertime aerosol transport is typically transported at lower altitudes as the height of emission for wintertime aerosols is lower compared to summertime aerosol transport, leading to greater mixing into the MBL (Tsamalis et al., 2013; Gutleben et al., 2022). Thus, smoke may be playing an important role in CCN formation throughout a large portion of the year. This is especially true considering the large size of long-range transported smoke plumes that have a wide geographic extent in which they can affect cloud formation. To conclude, this work highlights the need to characterize African smoke transport to Ragged Point and better understand the role of smoke in cloud formation, radiative forcing, and climate (Pechony and Shindell, 2010; Shindell et al., 2009).

Data availability. The data are publicly available in the University of Miami data repository: https://doi.org/10.17604/drt6-ys34 (Royer et al., 2022).

Supplement. The supplement related to this article is available online at: https://doi.org/10.5194/acp-23-981-2023-supplement.

Author contributions. Conceptualization of this work was done by HMR, MLP, OK, and CJG. Collection of samples was conducted by HMR, OK, EB, and PS, while analysis was done by HMR, MLP, OK, NNL, and ZC. The development of the methods used in this work was done by HMR, MLP, OK, ZC, SC, APA, and CJG. Instrumentation used to conduct this work was provided by MLP, SC, APA, and CJG. Formal analysis of data was performed by HMR, MLP, CP, and OK. Validation of data products was performed by HMR, ZC, SC, APA, and CJG. Computer code used for data analysis was provided by MLP, OK, and APA. Data visualization was performed by HMR, MLP, and OK. PKQ, PZ, CP, and UP helped interpret results. Supervision and project administration duties were done by MLP and CJG. HMR wrote the original draft for publication, and all the co-authors reviewed and edited this work.

Competing interests. At least one of the (co-)authors is a member of the editorial board of *Atmospheric Chemistry and Physics*. The peer-review process was guided by an independent editor, and the authors also have no other competing interests to declare.

Disclaimer. Publisher's note: Copernicus Publications remains neutral with regard to jurisdictional claims in published maps and institutional affiliations.

Acknowledgements. Cassandra J. Gaston received an NSF CAREER award (1944958). A portion of this research was performed on project awards (https://doi.org/10.46936/lser.proj.2019.50816/60000110 and https://doi.org/10.46936/lser.proj.2021.51900/60000361) from the Environmental Molecular Sciences Laboratory, a DOE Office of Science User Facility sponsored by the Biological and Environmental Research program under contract no. DE-AC05-76RL01830. Patricia K. Quinn was supported by PMEL contribution number 5353. Mira L. Pöhlker and Christopher Pöhlker were supported by the Max Planck Society. Paquita Zuidema was supported by NOAA grant OAR CPO NA19OAR4310379.

Financial support. This research has been supported by the Division of Atmospheric and Geospace Sciences (grant no. 1944958), the Environmental Molecular Sciences Laboratory (grant nos. 50816 and 51900), and the NOAA Pacific Marine Environmental Laboratory (grant no. 5353). Research was also supported by NOAA grant OAR CPO NA 19OAR4310379 and the Max Planck Society.

Review statement. This paper was edited by Markus Petters and reviewed by two anonymous referees.

References

Abel, S. J., Haywood, J. M., Highwood, E. J., Li, J., and Buseck, P. R.: Evolution of biomass burning aerosol properties from an agricultural fire in southern Africa, Geophys. Res. Lett., 30, 1783, https://doi.org/10.1029/2003GL017342, 2003.

Adams, A. M., Prospero, J. M., and Zhang, C.: CALIPSO-Derived Three-Dimensional Structure of Aerosol over the Atlantic Basin and Adjacent Continents, J. Climate, 25, 6862–6879, 2012.

Albrecht, B. A.: Aerosols, cloud microphysics, and fractional cloudiness, Science, 245, 1227–1230, https://doi.org/10.1126/science.245.4923.1227, 1989.

Allan, J. D., Baumgardner, D., Raga, G. B., Mayol-Bracero, O. L., Morales-García, F., García-García, F., Montero-Martínez, G., Borrmann, S., Schneider, J., Mertes, S., Walter, S., Gysel, M., Dusek, U., Frank, G. P., and Krämer, M.: Clouds and aerosols in Puerto Rico – a new evaluation, Atmos. Chem. Phys., 8, 1293–1309, https://doi.org/10.5194/acp-8-1293-2008, 2008.

Andreae, M. O.: Soot Carbon and Excess Fine Potassium: Long-Range Transport of Combustion-Derived Aerosols, Science, 220, 1148–1151, https://doi.org/10.1126/science.220.4602.1148, 1983.

Andreae, M. O.: Emission of trace gases and aerosols from biomass burning – an updated assessment, Atmos. Chem. Phys., 19, 8523–8546, https://doi.org/10.5194/acp-19-8523-2019, 2019.

Ansmann, A., Baars, H., Tesche, M., Müller, D., Althausen, D., Engelmann, R., Pauliquevis, T., and Artaxo, P.: Dust and smoke

transport from Africa to South America: Lidar profiling over Cape Verde and the Amazon rainforest, Geophys. Res. Lett., 36, L11802, https://doi.org/10.1029/2009GL037923, 2009.

Archibald, A. T., Witham, C. S., Ashfold, M. J., Manning, A. J., O'Doherty, S., Greally, B. R., Young, D., and Shallcross, D. E.: Long-term high frequency measurements of ethane, benzene and methyl chloride at Ragged Point, Barbados: Identification of long-range transport events, Elementa Science of the Anthropocene, 3, 000068, https://doi.org/10.12952/journal.elementa.000068, 2015.

Ault, A. P., Peters, T. M., Sawvel, E. J., Casuccio, G. S., Willis, R. D., Norris, G. A., and Grassian, V. H.: Single-Particle SEM-EDX Analysis of Iron-Containing Coarse Particulate Matter in an Urban Environment: Sources and Distribution of Iron within Cleveland, Ohio, Environ. Sci. Technol., 46, 4331–4339, https://doi.org/10.1021/es204006k, 2012.

Ault, A. P., Guasco, T. L., Ryder, O. S., Baltrusaitis, J., Cuadra-Rodriguez, L. A., Collins, D. B., Ruppel, M. J., Bertram, T. H., Prather, K. A., and Grassian, V. H.: Inside versus outside: Ion redistribution in nitric acid reacted sea spray aerosol particles as determined by single particle analysis, J. Am. Chem. Soc., 135, 14528–14531, https://doi.org/10.1021/ja407117x, 2013a.

Ault, A. P., Zhao, D., Ebben, C. J., Tauber, M. J., Geiger, F. M., Prather, K. A., and Grassian, V. H.: Raman microspectroscopy and vibrational sum frequency generation spectroscopy as probes of the bulk and surface compositions of size-resolved sea spray aerosol particles, Phys. Chem. Chem. Phys., 15, 6206–6214, https://doi.org/10.1039/C3CP43899F, 2013b.

Ault, A. P., Moffet, R. C., Baltrusaitis, J., Collins, D. B., Ruppel, M. J., Cuadra-Rodriguez, L. A., Zhao, D., Guasco, T. L., Ebben, C. J., Geiger, F. M., Bertram, T. H., Prather, K. A., and Grassian, V. H.: Size-Dependent Changes in Sea Spray Aerosol Composition and Properties with Different Seawater Conditions, Environ. Sci. Technol., 47, 5603–5612, https://doi.org/10.1021/es400416g, 2013c.

Ault, A. P., Guasco, T. L., Baltrusaitis, J., Ryder, O. S., Trueblood, J. V., Collins, D. B., Ruppel, M. J., Cuadra-Rodriguez, L. A., Prather, K. A., and Grassian, V. H.: Heterogeneous Reactivity of Nitric Acid with Nascent Sea Spray Aerosol: Large Differences Observed between and within Individual Particles, J. Phys. Chem. Lett., 5, 2493–2500, https://doi.org/10.1021/jz5008802, 2014.

Barkley, A. E., Prospero, J. M., Mahowald, N., Hamilton, D. S., Popendorf, K. J., Oehlert, A. M., Pourmand, A., Gatineau, A., Panechou-Pulcherie, K., Blackwelder, P., and Gaston, C. J.: African biomass burning is a substantial source of phosphorus deposition to the Amazon, Tropical Atlantic Ocean, and Southern Ocean, P. Natl. Acad. Sci. USA, 116, 16216–16221, https://doi.org/10.1073/pnas.1906091116, 2019.

Barkley, A. E., Olson, N. E., Prospero, J. M., Gatineau, A., Panechou, K., Maynard, N. G., Blackwelder, P., China, S., Ault, A. P., and Gaston, C. J.: Atmospheric Transport of North African Dust-Bearing Supermicron Freshwater Diatoms to South America: Implications for Iron Transport to the Equatorial North Atlantic Ocean, Geophys. Res. Lett., 48, e2020GL090476, https://doi.org/10.1029/2020GL090476, 2021.

Bates, T. S., Lamb, B. K., Guenther, A., Dignon, J., and Stoiber, R. E.: Sulfur emissions to the atmosphere from natural sourees, J. Atmos. Chem., 14, 315–337, https://doi.org/10.1007/BF00115242, 1992.

Behnke, W., George, C., Scheer, V., and Zetzsch, C.: Production and decay of $ClNO_2$ from the reaction of gaseous N_2O_5 with NaCl solution: Bulk and aerosol experiments, J. Geophys. Res.-Atmos., 102, 3795–3804, https://doi.org/10.1029/96jd03057, 1997.

Behrenfeld, M. J., Moore, R. H., Hostetler, C. A., Graff, J., Gaube, P., Russell, L. M., Chen, G., Doney, S. C., Giovannoni, S., Liu, H., Proctor, C., Bolaños, L. M., Baetge, N., Davie-Martin, C., Westberry, T. K., Bates, T. S., Bell, T. G., Bidle, K. D., Boss, E. S., Brooks, S. D., Cairns, B., Carlson, C., Halsey, K., Harvey, E. L., Hu, C., Karp-Boss, L., Kleb, M., Menden-Deuer, S., Morison, F., Quinn, P. K., Scarino, A. J., Anderson, B., Chowdhary, J., Crosbie, E., Ferrare, R., Hair, J. W., Hu, Y., Janz, S., Redemann, J., Saltzman, E., Shook, M., Siegel, D. A., Wisthaler, A., Martin, M. Y., and Ziemba, L.: The North Atlantic Aerosol and Marine Ecosystem Study (NAAMES): Science Motive and Mission Overview, Front. Mar. Sci., 6, 122, https://doi.org/10.3389/fmars.2019.00122, 2019.

Bondy, A. L., Bonanno, D., Moffet, R. C., Wang, B., Laskin, A., and Ault, A. P.: The diverse chemical mixing state of aerosol particles in the southeastern United States, Atmos. Chem. Phys., 18, 12595–12612, https://doi.org/10.5194/acp-18-12595-2018, 2018.

Capes, G., Johnson, B., McFiggans, G., Williams, P. I., Haywood, J., and Coe, H.: Aging of biomass burning aerosols over West Africa: Aircraft measurements of chemical composition, microphysical properties, and emission ratios, J. Geophys. Res.-Atmos., 113, D00C15, https://doi.org/10.1029/2008JD009845, 2008.

Cappa, C. D., Lim, C. Y., Hagan, D. H., Coggon, M., Koss, A., Sekimoto, K., de Gouw, J., Onasch, T. B., Warneke, C., and Kroll, J. H.: Biomass-burning-derived particles from a wide variety of fuels – Part 2: Effects of photochemical aging on particle optical and chemical properties, Atmos. Chem. Phys., 20, 8511–8532, https://doi.org/10.5194/acp-20-8511-2020, 2020.

Carlson, T. N. and Prospero, J. M.: The Large-Scale Movement of Saharan Air Outbreaks over the Northern Equatorial Atlantic, J. Appl. Meteorol. Clim., 11, 283–297, https://doi.org/10.1175/1520-0450(1972)011<0283:TLSMOS>2.0.CO;2, 1972.

Carslaw, K. S., Lee, L. A., Reddington, C. L., Pringle, K. J., Rap, A., Forster, P. M., Mann, G. W., Spracklen, D. v, Woodhouse, M. T., Regayre, L. A., and Pierce, J. R.: Large contribution of natural aerosols to uncertainty in indirect forcing, Nature, 503, 67–71, https://doi.org/10.1038/nature12674, 2013.

Chin, M., Diehl, T., Tan, Q., Prospero, J. M., Kahn, R. A., Remer, L. A., Yu, H., Sayer, A. M., Bian, H., Geogdzhayev, I. V., Holben, B. N., Howell, S. G., Huebert, B. J., Hsu, N. C., Kim, D., Kucsera, T. L., Levy, R. C., Mishchenko, M. I., Pan, X., Quinn, P. K., Schuster, G. L., Streets, D. G., Strode, S. A., Torres, O., and Zhao, X.-P.: Multi-decadal aerosol variations from 1980 to 2009: a perspective from observations and a global model, Atmos. Chem. Phys., 14, 3657–3690, https://doi.org/10.5194/acp-14-3657-2014, 2014.

Choël, M., Deboudt, K., Flament, P., Aimoz, L., and Mériaux, X.: Single-particle analysis of atmospheric aerosols at Cape Gris-Nez, English Channel: Influence of steel works

on iron apportionment, Atmos. Environ., 41, 2820–2830, https://doi.org/10.1016/j.atmosenv.2006.11.038, 2007.

Dang, C., Segal-Rozenhaimer, M., Che, H., Zhang, L., Formenti, P., Taylor, J., Dobracki, A., Purdue, S., Wong, P.-S., Nenes, A., Sedlacek III, A., Coe, H., Redemann, J., Zuidema, P., Howell, S., and Haywood, J.: Biomass burning and marine aerosol processing over the southeast Atlantic Ocean: a TEM single-particle analysis, Atmos. Chem. Phys., 22, 9389–9412, https://doi.org/10.5194/acp-22-9389-2022, 2022.

Deboudt, K., Flament, P., Choël, M., Gloter, A., Sobanska, S., and Colliex, C.: Mixing state of aerosols and direct observation of carbonaceous and marine coatings on African dust by individual particle analysis, J. Geophys. Res.-Atmos., 115, D24207, https://doi.org/10.1029/2010JD013921, 2010.

Denjean, C., Caquineau, S., Desboeufs, K., Laurent, B., Maille, M., Quiñones Rosado, M., Vallejo, P., Mayol-Bracero, O. L., and Formenti, P.: Long-range transport across the Atlantic in summertime does not enhance the hygroscopicity of African mineral dust, Geophys. Res. Lett., 42, 7835–7843, https://doi.org/10.1002/2015GL065693, 2015.

Dusek, U., Frank, G. P., Hildebrandt, L., Curtius, J., Schneider, J., Walter, S., Chand, D., Drewnick, F., Hings, S., Jung, D., Borrmann, S., and Andreae, M. O.: Size Matters More Than Chemistry for Cloud-Nucleating Ability of Aerosol Particles, Science, 312, 1375–1378, https://doi.org/10.1126/science.1125261, 2006.

Echalar, F., Gaudichet, A., Cachier, H., and Artaxo, P.: Aerosol emissions by tropical forest and savanna biomass burning: Characteristic trace elements and fluxes, Geophys. Res. Lett., 22, 3039–3042, https://doi.org/10.1029/95GL03170, 1995.

Edwards, E.-L., Corral, A. F., Dadashazar, H., Barkley, A. E., Gaston, C. J., Zuidema, P., and Sorooshian, A.: Impact of various air mass types on cloud condensation nuclei concentrations along coastal southeast Florida, Atmos. Environ., 254, 118371, https://doi.org/10.1016/j.atmosenv.2021.118371, 2021.

Forster, P., Storelvmo, T., Armour, K., Collins, W., Dufresne, J.-L., Frame, D., Lunt, D. J., Mauritsen, T., Palmer, M. D., Watanabe, M., Wild, M., and Zhang, H.: The Earth's Energy Budget, Climate Feedbacks, and Climate Sensitivity, in Climate Change 2021: The Physical Science Basis. Contribution of Working Group I to the Sixth Assessment Report of the Intergovernmental Panel on Climate Change, edited by: Masson-Delmotte, V., Zhai, P., Pirani, A., Connors, S. L., Péan, C., Berger, S., Caud, N., Chen, Y., Goldfarb, L., Gomis, M. I., Huang, M., Leitzell, K., Lonnoy, E., Matthews, J. B. R., Maycock, T. K., Waterfield, T., Yelekçi, O., Yu, R., and Zhou, B., Cambridge University Press, Cambridge, United Kingdom and New York, NY, USA, 923–1054, https://doi.org/10.1017/9781009157896.009, 2021.

Freney, E. J., Martin, S. T., and Buseck, P. R.: Deliquescence and efflorescence of potassium salts relevant to biomass-burning aerosol particles, Aerosol Sci. Tech., 43, 799–807, https://doi.org/10.1080/02786820902946620, 2009.

Gaston, C. J., Pratt, K. A., Qin, X., and Prather, K. A.: Real-time detection and mixing state of methanesulfonate in single particles at an inland urban location during a phytoplankton bloom, Environ. Sci. Technol., 44, 1566–1572, https://doi.org/10.1021/es902069d, 2010.

Gaston, C. J., Furutani, H., Guazzotti, S. A., Coffee, K. R., Bates, T. S., Quinn, P. K., Aluwihare, L. I., Mitchell, B. G., and Prather, K. A.: Unique ocean-derived particles serve as a proxy for changes in ocean chemistry, J. Geophys. Res.-Atmos., 116, 1–13, https://doi.org/10.1029/2010JD015289, 2011.

Gaston, C. J., Quinn, P. K., Bates, T. S., Gilman, J. B., Bon, D. M., Kuster, W. C., and Prather, K. A.: The impact of shipping, agricultural, and urban emissions on single particle chemistry observed aboard the R/V Atlantis during CalNex, J. Geophys. Res.-Atmos., 118, 5003–5017, https://doi.org/10.1002/jgrd.50427, 2013.

Giordano, M., Espinoza, C., and Asa-Awuku, A.: Experimentally measured morphology of biomass burning aerosol and its impacts on CCN ability, Atmos. Chem. Phys., 15, 1807–1821, https://doi.org/10.5194/acp-15-1807-2015, 2015.

Good, N., Topping, D. O., Allan, J. D., Flynn, M., Fuentes, E., Irwin, M., Williams, P. I., Coe, H., and McFiggans, G.: Consistency between parameterisations of aerosol hygroscopicity and CCN activity during the RHaMBLe discovery cruise, Atmos. Chem. Phys., 10, 3189–3203, https://doi.org/10.5194/acp-10-3189-2010, 2010.

Gutleben, M., Groß, S., Heske, C., and Wirth, M.: Wintertime Saharan dust transport towards the Caribbean: an airborne lidar case study during EUREC^{4}A, Atmos. Chem. Phys., 22, 7319–7330, https://doi.org/10.5194/acp-22-7319-2022, 2022.

Hand, V. L., Capes, G., Vaughan, D. J., Formenti, P., Haywood, J. M., and Coe, H.: Evidence of internal mixing of African dust and biomass burning particles by individual particle analysis using electron beam techniques, J. Geophys. Res.-Atmos., 115, D13301, https://doi.org/10.1029/2009JD012938, 2010.

Hennigan, C. J., Sullivan, A. P., Collett Jr., J. L., and Robinson, A. L.: Levoglucosan stability in biomass burning particles exposed to hydroxyl radicals, Geophys. Res. Lett., 37, L09806, https://doi.org/10.1029/2010GL043088, 2010.

Hennigan, C. J., Miracolo, M. A., Engelhart, G. J., May, A. A., Presto, A. A., Lee, T., Sullivan, A. P., McMeeking, G. R., Coe, H., Wold, C. E., Hao, W.-M., Gilman, J. B., Kuster, W. C., de Gouw, J., Schichtel, B. A., Collett Jr., J. L., Kreidenweis, S. M., and Robinson, A. L.: Chemical and physical transformations of organic aerosol from the photo-oxidation of open biomass burning emissions in an environmental chamber, Atmos. Chem. Phys., 11, 7669–7686, https://doi.org/10.5194/acp-11-7669-2011, 2011.

Hodshire, A. L., Akherati, A., Alvarado, M. J., Brown-Steiner, B., Jathar, S. H., Jimenez, J. L., Kreidenweis, S. M., Lonsdale, C. R., Onasch, T. B., Ortega, A. M., and Pierce, J. R.: Aging Effects on Biomass Burning Aerosol Mass and Composition: A Critical Review of Field and Laboratory Studies, Environ. Sci. Technol., 53, 10007–10022, https://doi.org/10.1021/acs.est.9b02588, 2019.

Hoffman, R. C., Laskin, A., and Finlayson-Pitts, B. J.: Sodium nitrate particles: physical and chemical properties during hydration and dehydration, and implications for aged sea salt aerosols, J. Aerosol. Sci., 35, 869–887, https://doi.org/10.1016/j.jaerosci.2004.02.003, 2004.

Holanda, B. A., Pöhlker, M. L., Walter, D., Saturno, J., Sörgel, M., Ditas, J., Ditas, F., Schulz, C., Franco, M. A., Wang, Q., Donth, T., Artaxo, P., Barbosa, H. M. J., Borrmann, S., Braga, R., Brito, J., Cheng, Y., Dollner, M., Kaiser, J. W., Klimach, T., Knote, C., Krüger, O. O., Fütterer, D., Lavrič, J. V., Ma, N., Machado, L. A. T., Ming, J., Morais, F. G., Paulsen, H., Sauer, D., Schlager, H., Schneider, J., Su, H., Weinzierl, B., Walser, A., Wendisch, M., Ziereis, H., Zöger, M., Pöschl, U., Andreae, M. O., and Pöh-

lker, C.: Influx of African biomass burning aerosol during the Amazonian dry season through layered transatlantic transport of black carbon-rich smoke, Atmos. Chem. Phys., 20, 4757–4785, https://doi.org/10.5194/acp-20-4757-2020, 2020.

Hoppel, W. A., Frick, G. M., and Larson, R. E.: Effect of nonprecipitating clouds on the aerosol size distribution in the marine boundary layer, Geophys. Res. Lett., 13, 125–128, https://doi.org/10.1029/GL013i002p00125, 1986.

Hudson, P. K., Murphy, D. M., Cziczo, D. J., Thomson, D. S., de Gouw, J. A., Warneke, C., Holloway, J., Jost, H.-J., and Hübler, G.: Biomass-burning particle measurements: Characteristic composition and chemical processing, J. Geophys. Res.-Atmos., 109, D23S27, https://doi.org/10.1029/2003JD004398, 2004.

Kacarab, M., Thornhill, K. L., Dobracki, A., Howell, S. G., O'Brien, J. R., Freitag, S., Poellot, M. R., Wood, R., Zuidema, P., Redemann, J., and Nenes, A.: Biomass burning aerosol as a modulator of the droplet number in the southeast Atlantic region, Atmos. Chem. Phys., 20, 3029–3040, https://doi.org/10.5194/acp-20-3029-2020, 2020.

Kitto, M. E. and Anderson, D. L.: The use of Whatman-41 filters for particle, Atmos. Environ., 22, 2629–2630, https://doi.org/10.1016/0004-6981(88)90500-8, 1988.

Klingebiel, M., Ghate, V. P., Naumann, A. K., Ditas, F., Pöhlker, M. L., Pöhlker, C., Kandler, K., Konow, H., and Stevens, B.: Remote Sensing of Sea Salt Aerosol below Trade Wind Clouds, J. Atmos. Sci., 76, 1189–1202, https://doi.org/10.1175/JAS-D-18-0139.1, 2019.

Konovalov, I. B., Golovushkin, N. A., Beekmann, M., and Andreae, M. O.: Insights into the aging of biomass burning aerosol from satellite observations and 3D atmospheric modeling: evolution of the aerosol optical properties in Siberian wildfire plumes, Atmos. Chem. Phys., 21, 357–392, https://doi.org/10.5194/acp-21-357-2021, 2021.

Kristensen, T. B., Müller, T., Kandler, K., Benker, N., Hartmann, M., Prospero, J. M., Wiedensohler, A., and Stratmann, F.: Properties of cloud condensation nuclei (CCN) in the trade wind marine boundary layer of the western North Atlantic, Atmos. Chem. Phys., 16, 2675–2688, https://doi.org/10.5194/acp-16-2675-2016, 2016.

Krueger, B. J., Grassian, V. H., Cowin, J. P., and Laskin, A.: Heterogeneous chemistry of individual mineral dust particles from different dust source regions: the importance of particle mineralogy, Atmos. Environ., 38, 6253–6261, https://doi.org/10.1016/j.atmosenv.2004.07.010, 2004.

Laskin, A., Wietsma, T. W., Krueger, B. J., and Grassian, V. H.: Heterogeneous chemistry of individual mineral dust particles with nitric acid: A combined CCSEM/EDX, ESEM, and ICP-MS study, J. Geophys. Res.-Atmos., 110, D10208, https://doi.org/10.1029/2004JD005206, 2005.

Laskin, A., Moffet, R. C., Gilles, M. K., Fast, J. D., Zaveri, R. A., Wang, B., Nigge, P., and Shutthanandan, J.: Tropospheric chemistry of internally mixed sea salt and organic particles: Surprising reactivity of NaCl with weak organic acids, J. Geophys. Res.-Atmos., 117, D15302, https://doi.org/10.1029/2012JD017743, 2012.

Lathem, T. L., Beyersdorf, A. J., Thornhill, K. L., Winstead, E. L., Cubison, M. J., Hecobian, A., Jimenez, J. L., Weber, R. J., Anderson, B. E., and Nenes, A.: Analysis of CCN activity of Arctic aerosol and Canadian biomass burning during summer 2008, Atmos. Chem. Phys., 13, 2735–2756, https://doi.org/10.5194/acp-13-2735-2013, 2013.

Levin, Z., Teller, A., Ganor, E., and Yin, Y.: On the interactions of mineral dust, sea-salt particles, and clouds: A measurement and modeling study from the Mediterranean Israeli Dust Experiment campaign, J. Geophys. Res.-Atmos., 110, D20202, https://doi.org/10.1029/2005JD005810, 2005.

Li, J., Pósfai, M., Hobbs, P. V., and Buseck, P. R.: Individual aerosol particles from biomass burning in southern Africa: 2, Compositions and aging of inorganic particles, J. Geophys. Res.-Atmos., 108, 8484, https://doi.org/10.1029/2002JD002310, 2003.

Li, W., Shao, L., Wang, Z., Shen, R., Yang, S., and Tang, U.: Size, composition, and mixing state of individual aerosol particles in a South China coastal city, J. Environ. Sci., 22, 561–569, https://doi.org/10.1016/S1001-0742(09)60146-7, 2010.

Maenhaut, W., Salma, I., Cafmeyer, J., Annegarn, H. J., and Andreae, M. O.: Regional atmospheric aerosol composition and sources in the eastern Transvaal, South Africa, and impact of biomass burning, J. Geophys. Res.-Atmos., 101, 23631–23650, https://doi.org/10.1029/95JD02930, 1996.

McCoy, D. T., Burrows, S. M., Wood, R., Grosvenor, D. P., Elliott, S. M., Ma, P.-L., Rasch, P. J., and Hartment, D. L.: Natural aerosols explain seasonal and spatial patterns of Southern Ocean cloud albedo, Sci. Adv., 1, e1500157, https://doi.org/10.1126/sciadv.1500157, 2022.

McFiggans, G., Artaxo, P., Baltensperger, U., Coe, H., Facchini, M. C., Feingold, G., Fuzzi, S., Gysel, M., Laaksonen, A., Lohmann, U., Mentel, T. F., Murphy, D. M., O'Dowd, C. D., Snider, J. R., and Weingartner, E.: The effect of physical and chemical aerosol properties on warm cloud droplet activation, Atmos. Chem. Phys., 6, 2593–2649, https://doi.org/10.5194/acp-6-2593-2006, 2006.

Miles, J. C., Crutzen, P. J., and Goldammer, J. G.: Fire in the Environment: The Ecological, Atmospheric, and Climatic Importance of Vegetation Fires, Report of the Dahlem Workshop held in Berlin, 15-20 March 1992, Wiley, Chichester, England, 400 pp., 0-471-93604-9, 1993.

Miller, R. M., McFarquhar, G. M., Rauber, R. M., O'Brien, J. R., Gupta, S., Segal-Rozenhaimer, M., Dobracki, A. N., Sedlacek, A. J., Burton, S. P., Howell, S. G., Freitag, S., and Dang, C.: Observations of supermicron-sized aerosols originating from biomass burning in southern Central Africa, Atmos. Chem. Phys., 21, 14815–14831, https://doi.org/10.5194/acp-21-14815-2021, 2021.

Moran-Zuloaga, D., Ditas, F., Walter, D., Saturno, J., Brito, J., Carbone, S., Chi, X., Hrabě de Angelis, I., Baars, H., Godoi, R. H. M., Heese, B., Holanda, B. A., Lavrič, J. V., Martin, S. T., Ming, J., Pöhlker, M. L., Ruckteschler, N., Su, H., Wang, Y., Wang, Q., Wang, Z., Weber, B., Wolff, S., Artaxo, P., Pöschl, U., Andreae, M. O., and Pöhlker, C.: Long-term study on coarse mode aerosols in the Amazon rain forest with the frequent intrusion of Saharan dust plumes, Atmos. Chem. Phys., 18, 10055–10088, https://doi.org/10.5194/acp-18-10055-2018, 2018.

Murphy, D. M., Cziczo, D. J., Froyd, K. D., Hudson, P. K., Matthew, B. M., Middlebrook, A. M., Peltier, R. E., Sullivan, A., Thomson, D. S., and Weber, R. J.: Single-particle mass spectrometry of tropospheric aerosol particles, J. Geophys. Res.-Atmos., 111, D23S32, https://doi.org/10.1029/2006JD007340, 2006.

Nájera, J. J. and Horn, A. B.: Infrared spectroscopic study of the effect of oleic acid on the deliquescence behaviour of ammonium sulfate aerosol particles, Phys. Chem. Chem. Phys., 11, 483–494, https://doi.org/10.1039/B812182F, 2009.

O'Dowd, C. D. and de Leeuw, G.: Marine aerosol production: a review of the current knowledge, Philosophical Transactions of the Royal Society A: Mathematical, Phys. Eng. Sci., 365, 1753–1774, https://doi.org/10.1098/rsta.2007.2043, 2007.

O'Dowd, C. D., Facchini, M. C., Cavalli, F., Ceburnis, D., Mircea, M., Decesari, S., Fuzzi, S., Yoon, Y. J., and Putaud, J.-P.: Biogenically driven organic contribution to marine aerosol, Nature, 431, 676–680, https://doi.org/10.1038/nature02959, 2004.

Pachauri, T., Singla, V., Satsangi, A., Lakhani Anita, and Kumari, K. M.: SEM-EDX Characterization of Individual Coarse Particles in Agra, India, Aerosol Air Qual. Res., 13, 523–536, https://doi.org/10.4209/aaqr.2012.04.0095, 2013.

Petters, M. D. and Kreidenweis, S. M.: A single parameter representation of hygroscopic growth and cloud condensation nucleus activity, Atmos. Chem. Phys., 7, 1961–1971, https://doi.org/10.5194/acp-7-1961-2007, 2007.

Pierce, J. R., Chen, K., and Adams, P. J.: Contribution of primary carbonaceous aerosol to cloud condensation nuclei: processes and uncertainties evaluated with a global aerosol microphysics model, Atmos. Chem. Phys., 7, 5447–5466, https://doi.org/10.5194/acp-7-5447-2007, 2007.

Pósfai, M., Simonics, R., Li, J., Hobbs, P. v, and Buseck, P. R.: Individual aerosol particles from biomass burning in southern Africa: 1. Compositions and size distributions of carbonaceous particles, J. Geophys. Res.-Atmos., 108, 8483, https://doi.org/10.1029/2002JD002291, 2003.

Prospero, J. M.: atmospheric dust studies on Barbados, B. Am. Meteorol. Soc., 49, 645–652, https://doi.org/10.1175/1520-0477-49.6.645, 1968.

Prospero, J. M.: Long-range transport of mineral dust in the global atmosphere: Impact of African dust on the environment of the southeastern United States, P. Natl. Acad. Sci. USA, 96, 3396–3403, https://doi.org/10.1073/pnas.96.7.3396, 1999.

Prospero, J. M. and Lamb, P. J.: African Droughts and Dust Transport to the Caribbean: Climate Change Implications, Science, 302, 1024–1027, https://doi.org/10.1126/science.1089915, 2003.

Prospero, J. M. and Mayol-Bracero, O. L.: Understanding the Transport and Impact of African Dust on the Caribbean Basin, B. Am. Meteorol. Soc., 94, 1329–1337, https://doi.org/10.1175/BAMS-D-12-00142.1, 2013.

Prospero, J. M., Glaccum, R. A., and Nees, R. T.: Atmospheric transport of soil dust from Africa to South America, Nature, 289, 570–572, https://doi.org/10.1038/289570a0, 1981.

Prospero, J. M., Blades, E., Mathison, G., and Naidu, R.: Interhemispheric transport of viable fungi and bacteria from Africa to the Caribbean with soil dust, Aerobiologia, 21, 1–19, https://doi.org/10.1007/s10453-004-5872-7, 2005.

Prospero, J. M., Collard, F.-X., Molinié, J., and Jeannot, A.: Characterizing the annual cycle of African dust transport to the Caribbean Basin and South America and its impact on the environment and air quality, Global Biogeochem. Cy., 28, 757–773, https://doi.org/10.1002/2013GB004802, 2014.

Prospero, J. M., Barkley, A. E., Gaston, C. J., Gatineau, A., Campos y Sansano, A., and Panechou, K.: Characterizing and Quantifying African Dust Transport and Deposition to South America: Implications for the Phosphorus Budget in the Amazon Basin, Global Biogeochem. Cy., 34, e2020GB006536, https://doi.org/10.1029/2020GB006536, 2020.

Prospero, J. M., Delany, A. C., Delany, A. C., and Carlson, T. N.: The Discovery of African Dust Transport to the Western Hemisphere and the Saharan Air Layer: A History, B. Am. Meteorol. Soc., 102, 1239–1260, https://doi.org/10.1175/BAMS-D-19-0309.1, 2021.

Pszenny, A., Fischer, C., Mendez, A., and Zetwo, M.: Direct comparison of cellulose and quartz fiber filters for sampling submicrometer aerosols in the marine boundary layer, Atmos. Environ., 27, 281–284, https://doi.org/10.1016/0960-1686(93)90359-7, 1993.

Quinn, P. K., Bates, T. S., Coffman, D. J., and Covert, D. S.: Influence of particle size and chemistry on the cloud nucleating properties of aerosols, Atmos. Chem. Phys., 8, 1029–1042, https://doi.org/10.5194/acp-8-1029-2008, 2008.

Quinn, P. K., Thompson, E. J., Coffman, D. J., Baidar, S., Bariteau, L., Bates, T. S., Bigorre, S., Brewer, A., de Boer, G., de Szoeke, S. P., Drushka, K., Foltz, G. R., Intrieri, J., Iyer, S., Fairall, C. W., Gaston, C. J., Jansen, F., Johnson, J. E., Krüger, O. O., Marchbanks, R. D., Moran, K. P., Noone, D., Pezoa, S., Pincus, R., Plueddemann, A. J., Pöhlker, M. L., Pöschl, U., Quinones Melendez, E., Royer, H. M., Szczodrak, M., Thomson, J., Upchurch, L. M., Zhang, C., Zhang, D., and Zuidema, P.: Measurements from the RV Ronald H. Brown and related platforms as part of the Atlantic Tradewind Ocean-Atmosphere Mesoscale Interaction Campaign (ATOMIC), Earth Syst. Sci. Data, 13, 1759–1790, https://doi.org/10.5194/essd-13-1759-2021, 2021.

Rauber, R. M., Stevens, B., Ochs, H. T., Knight, C., Albrecht, B. A., Blyth, A. M., Fairall, C. W., Jensen, J. B., Lasher-Trapp, S. G., Mayol-Bracero, O. L., Vali, G., Anderson, J. R., Baker, B. A., Bandy, A. R., Burnet, E., Brenguier, J.-L., Brewer, W. A., Brown, P. R. A., Chuang, R., Cotton, W. R., di Girolamo, L., Geerts, B., Gerber, H., Göke, S., Gomes, L., Heikes, B. G., Hudson, J. G., Kollias, P., Lawson, R. R., Krueger, S. K., Lenschow, D. H., Nuijens, L., O'Sullivan, D. W., Rilling, R. A., Rogers, D. C., Siebesma, A. P., Snodgrass, E., Stith, J. L., Thornton, D. C., Tucker, S., Twohy, C. H., and Zuidema, P.: Rain in Shallow Cumulus Over the Ocean: The RICO Campaign, B. Am. Meteorol. Soc., 88, 1912–1928, https://doi.org/10.1175/BAMS-88-12-1912, 2007.

Reid, J. S., Hobbs, P. v, Ferek, R. J., Blake, D. R., Martins, J. V., Dunlap, M. R., and Liousse, C.: Physical, chemical, and optical properties of regional hazes dominated by smoke in Brazil, J. Geophys. Res.-Atmos., 103, 32059–32080, https://doi.org/10.1029/98JD00458, 1998.

Reid, J. S., Koppmann, R., Eck, T. F., and Eleuterio, D. P.: A review of biomass burning emissions part II: intensive physical properties of biomass burning particles, Atmos. Chem. Phys., 5, 799–825, https://doi.org/10.5194/acp-5-799-2005, 2005.

Remoundaki, E., Bourliva, A., Kokkalis, P., Mamouri, R. E., Papayannis, A., Grigoratos, T., Samara, C., and Tsezos, M.: PM_{10} composition during an intense Saharan dust transport event over Athens (Greece), Sci. Total Environ., 409, 4361–4372, https://doi.org/10.1016/j.scitotenv.2011.06.026, 2011.

Roberts, G., Wooster, M. J., and Lagoudakis, E.: Annual and diurnal african biomass burning temporal dynamics, Biogeosciences, 6, 849–866, https://doi.org/10.5194/bg-6-849-2009, 2009.

Roberts, G. C. and Nenes, A.: A Continuous-Flow Streamwise Thermal-Gradient CCN Chamber for Atmospheric Measurements, Aerosol. Sci. Tech., 39, 206–221, https://doi.org/10.1080/027868290913988, 2005.

Roberts, G. C., Artaxo, P., Zhou, J., Swietlicki, E., and Andreae, M. O.: Sensitivity of CCN spectra on chemical and physical properties of aerosol: A case study from the Amazon Basin, J. Geophys. Res.-Atmos., 107, 37–18, https://doi.org/10.1029/2001JD000583, 2002.

Rogers, C. F., Hudson, J. G., Zielinska, B., Tanner, R. L., Hallett, J., Watson, J. G., and Levine, J. S. (Ed.): Cloud condensation nuclei from biomass burning. United States: Massachusetts Inst of Tech Press, 1991.

Rolph, G., Stein, A., and Stunder, B.: Real-time Environmental Applications and Display sYstem: READY, Environ. Model. Softw., 95, 210–228, https://doi.org/10.1016/j.envsoft.2017.06.025, 2017.

Rose, D., Gunthe, S. S., Mikhailov, E., Frank, G. P., Dusek, U., Andreae, M. O., and Pöschl, U.: Calibration and measurement uncertainties of a continuous-flow cloud condensation nuclei counter (DMT-CCNC): CCN activation of ammonium sulfate and sodium chloride aerosol particles in theory and experiment, Atmos. Chem. Phys., 8, 1153–1179, https://doi.org/10.5194/acp-8-1153-2008, 2008.

Rosenfeld, D., Rudich, Y., and Lahav, R.: Desert dust suppressing precipitation: A possible desertification feedback loop, P. Natl. Acad. Sci. USA, 98, 5975–5980, https://doi.org/10.1073/pnas.101122798, 2001.

Royer, H., Pöhlker, M., Krueger, O. O., Blades, E., Sealy, P., Lata, N. N., Cheng, Z., China, S., Ault, A., Quinn, P., Zuidema, P., Pöhlker, C., Pöschl, U., Andreae, M., and Gaston, C.: African smoke particles act as cloud condensation nuclei in the wintertime tropical North Atlantic boundary layer over Barbados, [data set], University of Miami Libraries, https://doi.org/10.17604/DRT6-YS34, last access: 13 January 2023.

Russell, L. M., Hawkins, L. N., Frossard, A. A., Quinn, P. K., and Bates, T. S.: Carbohydrate-like composition of submicron atmospheric particles and their production from ocean bubble bursting, P. Natl. Acad. Sci. USA, 107, 6652–6657, https://doi.org/10.1073/pnas.0908905107, 2010.

Savoie, D. L., Arimoto, R., Keene, W. C., Prospero, J. M., Duce, R. A., and Galloway, J. N.: Marine biogenic and anthropogenic contributions to non-sea-salt sulfate in the marine boundary layer over the North Atlantic Ocean, J. Geophys. Res.-Atmos., 107, 3–21, https://doi.org/10.1029/2001JD000970, 2002.

Schill, G. P., Froyd, K. D., Bian, H., Kupc, A., Williamson, C., Brock, C. A., Ray, E., Hornbrook, R. S., Hills, A. J., Apel, E. C., Chin, M., Colarco, P. R., and Murphy, D. M.: Widespread biomass burning smoke throughout the remote troposphere, Nat. Geosci., 13, 422–427, https://doi.org/10.1038/s41561-020-0586-1, 2020.

Shen, H., Peters, T. M., Casuccio, G. S., Lersch, T. L., West, R. R., Kumar, A., Kumar, N., and Ault, A. P.: Elevated Concentrations of Lead in Particulate Matter on the Neighborhood-Scale in Delhi, India As Determined by Single Particle Analysis, Environ. Sci. Technol., 50, 4961–4970, https://doi.org/10.1021/acs.est.5b06202, 2016.

Sobanska, S., Coeur, C., Maenhaut, W., and Adams, F.: SEM-EDX Characterisation of Tropospheric Aerosols in the Negev Desert (Israel), J. Atmos. Chem., 44, 299–322, https://doi.org/10.1023/A:1022969302107, 2003.

Sobanska, S., Falgayrac, G., Rimetz-Planchon, J., Perdrix, E., Brémard, C., and Barbillat, J.: Resolving the internal structure of individual atmospheric aerosol particle by the combination of Atomic Force Microscopy, ESEM–EDX, Raman and ToF–SIMS imaging, Microchem. J., 114, 89–98, https://doi.org/10.1016/j.microc.2013.12.007, 2014.

Sorooshian, A., Corral, A. F., Braun, R. A., Cairns, B., Crosbie, E., Ferrare, R., Hair, J., Kleb, M. M., Hossein Mardi, A., Maring, H., McComiskey, A., Moore, R., Painemal, D., Scarino, A. J., Schlosser, J., Shingler, T., Shook, M., Wang, H., Zeng, X., Ziemba, L., and Zuidema, P.: Atmospheric Research Over the Western North Atlantic Ocean Region and North American East Coast: A Review of Past Work and Challenges Ahead, J. Geophys. Res.-Atmos., 125, e2019JD031626, https://doi.org/10.1029/2019JD031626, 2020.

Spracklen, D. V., Carslaw, K. S., Pöschl, U., Rap, A., and Forster, P. M.: Global cloud condensation nuclei influenced by carbonaceous combustion aerosol, Atmos. Chem. Phys., 11, 9067–9087, https://doi.org/10.5194/acp-11-9067-2011, 2011.

Stein, A. F., Draxler, R. R., Rolph, G. D., Stunder, B. J. B., Cohen, M. D., and Ngan, F.: NOAA's HYSPLIT Atmospheric Transport and Dispersion Modeling System, B. Am. Meteorol. Soc., 96, 2059–2077, https://doi.org/10.1175/BAMS-D-14-00110.1, 2015.

Stevens, B., Farrell, D., Hirsch, L., Jansen, F., Nuijens, L., Serikov, I., Brügmann, B., Forde, M., Linne, H., Lonitz, K., and Prospero, J. M.: The Barbados Cloud Observatory: Anchoring Investigations of Clouds and Circulation on the Edge of the ITCZ, B. Am. Meteorol. Soc., 97, 787–801, https://doi.org/10.1175/BAMS-D-14-00247.1, 2016.

Stevens, B., Bony, S., Farrell, D., Ament, F., Blyth, A., Fairall, C., Karstensen, J., Quinn, P. K., Speich, S., Acquistapace, C., Aemisegger, F., Albright, A. L., Bellenger, H., Bodenschatz, E., Caesar, K.-A., Chewitt-Lucas, R., de Boer, G., Delanoë, J., Denby, L., Ewald, F., Fildier, B., Forde, M., George, G., Gross, S., Hagen, M., Hausold, A., Heywood, K. J., Hirsch, L., Jacob, M., Jansen, F., Kinne, S., Klocke, D., Kölling, T., Konow, H., Lothon, M., Mohr, W., Naumann, A. K., Nuijens, L., Olivier, L., Pincus, R., Pöhlker, M., Reverdin, G., Roberts, G., Schnitt, S., Schulz, H., Siebesma, A. P., Stephan, C. C., Sullivan, P., Touzé-Peiffer, L., Vial, J., Vogel, R., Zuidema, P., Alexander, N., Alves, L., Arixi, S., Asmath, H., Bagheri, G., Baier, K., Bailey, A., Baranowski, D., Baron, A., Barrau, S., Barrett, P. A., Batier, F., Behrendt, A., Bendinger, A., Beucher, F., Bigorre, S., Blades, E., Blossey, P., Bock, O., Böing, S., Bosser, P., Bourras, D., Bouruet-Aubertot, P., Bower, K., Branellec, P., Branger, H., Brennek, M., Brewer, A., Brilouet , P.-E., Brügmann, B., Buehler, S. A., Burke, E., Burton, R., Calmer, R., Canonici, J.-C., Carton, X., Cato Jr., G., Charles, J. A., Chazette, P., Chen, Y., Chilinski, M. T., Choularton, T., Chuang, P., Clarke, S., Coe, H., Cornet, C., Coutris, P., Couvreux, F., Crewell, S., Cronin, T., Cui, Z., Cuypers, Y., Daley, A., Damerell, G. M., Dauhut, T., Deneke, H., Desbios, J.-P., Dörner, S., Donner, S., Douet, V., Drushka, K., Dütsch, M., Ehrlich, A., Emanuel, K., Emmanouilidis, A., Etienne, J.-C., Etienne-Leblanc, S., Faure, G., Feingold, G., Ferrero, L., Fix, A., Flamant, C., Flatau, P. J., Foltz, G. R., Forster, L., Furtuna, I., Gadian, A., Galewsky, J., Gallagher, M., Gallimore,

P., Gaston, C., Gentemann, C., Geyskens, N., Giez, A., Gollop, J., Gouirand, I., Gourbeyre, C., de Graaf, D., de Groot, G. E., Grosz, R., Güttler, J., Gutleben, M., Hall, K., Harris, G., Helfer, K. C., Henze, D., Herbert, C., Holanda, B., Ibanez-Landeta, A., Intrieri, J., Iyer, S., Julien, F., Kalesse, H., Kazil, J., Kellman, A., Kidane, A. T., Kirchner, U., Klingebiel, M., Körner, M., Kremper, L. A., Kretzschmar, J., Krüger, O., Kumala, W., Kurz, A., L'Hégaret, P., Labaste, M., Lachlan-Cope, T., Laing, A., Landschützer, P., Lang, T., Lange, D., Lange, I., Laplace, C., Lavik, G., Laxenaire, R., Le Bihan, C., Leandro, M., Lefevre, N., Lena, M., Lenschow, D., Li, Q., Lloyd, G., Los, S., Losi, N., Lovell, O., Luneau, C., Makuch, P., Malinowski, S., Manta, G., Marinou, E., Marsden, N., Masson, S., Maury, N., Mayer, B., Mayers-Als, M., Mazel, C., McGeary, W., McWilliams, J. C., Mech, M., Mehlmann, M., Meroni, A. N., Mieslinger, T., Minikin, A., Minnett, P., Möller, G., Morfa Avalos, Y., Muller, C., Musat, I., Napoli, A., Neuberger, A., Noisel, C., Noone, D., Nordsiek, F., Nowak, J. L., Oswald, L., Parker, D. J., Peck, C., Person, R., Philippi, M., Plueddemann, A., Pöhlker, C., Pörtge, V., Pöschl, U., Pologne, L., Posyniak, M., Prange, M., Quiñones Meléndez, E., Radtke, J., Ramage, K., Reimann, J., Renault, L., Reus, K., Reyes, A., Ribbe, J., Ringel, M., Ritschel, M., Rocha, C. B., Rochetin, N., Röttenbacher, J., Rollo, C., Royer, H., Sadoulet, P., Saffin, L., Sandiford, S., Sandu, I., Schäfer, M., Schemann, V., Schirmacher, I., Schlenczek, O., Schmidt, J., Schröder, M., Schwarzenboeck, A., Sealy, A., Senff, C. J., Serikov, I., Shohan, S., Siddle, E., Smirnov, A., Späth, F., Spooner, B., Stolla, M. K., Szkółka, W., de Szoeke, S. P., Tarot, S., Tetoni, E., Thompson, E., Thomson, J., Tomassini, L., Totems, J., Ubele, A. A., Villiger, L., von Arx, J., Wagner, T., Walther, A., Webber, B., Wendisch, M., Whitehall, S., Wiltshire, A., Wing, A. A., Wirth, M., Wiskandt, J., Wolf, K., Worbes, L., Wright, E., Wulfmeyer, V., Young, S., Zhang, C., Zhang, D., Ziemen, F., Zinner, T., and Zöger, M.: EUREC^{4}A, Earth Syst. Sci. Data, 13, 4067–4119, https://doi.org/10.5194/essd-13-4067-2021, 2021.

Talbot, R. W., Andreae, M. O., Berresheim, H., Artaxo, P., Garstang, M., Harriss, R. C., Beecher, K. M., and Li, S. M.: Aerosol chemistry during the wet season in central Amazonia: The influence of long-range transport, J. Geophys. Res.-Atmos., 95, 16955–16969, https://doi.org/10.1029/JD095iD10p16955, 1990.

Tomlin, J. M., Jankowski, K. A., Veghte, D. P., China, S., Wang, P., Fraund, M., Weis, J., Zheng, G., Wang, Y., Rivera-Adorno, F., Raveh-Rubin, S., Knopf, D. A., Wang, J., Gilles, M. K., Moffet, R. C., and Laskin, A.: Impact of dry intrusion events on the composition and mixing state of particles during the winter Aerosol and Cloud Experiment in the Eastern North Atlantic (ACE-ENA), Atmos. Chem. Phys., 21, 18123–18146, https://doi.org/10.5194/acp-21-18123-2021, 2021.

Tsamalis, C., Chédin, A., Pelon, J., and Capelle, V.: The seasonal vertical distribution of the Saharan Air Layer and its modulation by the wind, Atmos. Chem. Phys., 13, 11235–11257, https://doi.org/10.5194/acp-13-11235-2013, 2013.

Twohy, C. H., Kreidenweis, S. M., Eidhammer, T., Browell, E. v., Heymsfield, A. J., Bansemer, A. R., Anderson, B. E., Chen, G., Ismail, S., DeMott, P. J., and van den Heever, S. C.: Saharan dust particles nucleate droplets in eastern Atlantic clouds, Geophys. Res. Lett., 36, L01807, https://doi.org/10.1029/2008GL035846, 2009.

Twomey, S.: Pollution and the planetary albedo, Atmos. Environ., 8, 1251–1256, https://doi.org/10.1016/0004-6981(74)90004-3, 1974.

Twomey, S.: The Influence of Pollution on the Shortwave Albedo of Clouds, J. Atmos. Sci., 34, 1149–1152, 1977.

Wang, Q., Saturno, J., Chi, X., Walter, D., Lavric, J. V., Moran-Zuloaga, D., Ditas, F., Pöhlker, C., Brito, J., Carbone, S., Artaxo, P., and Andreae, M. O.: Modeling investigation of light-absorbing aerosols in the Amazon Basin during the wet season, Atmos. Chem. Phys., 16, 14775–14794, https://doi.org/10.5194/acp-16-14775-2016, 2016.

Wex, H., Dieckmann, K., Roberts, G. C., Conrath, T., Izaguirre, M. A., Hartmann, S., Herenz, P., Schäfer, M., Ditas, F., Schmeissner, T., Henning, S., Wehner, B., Siebert, H., and Stratmann, F.: Aerosol arriving on the Caribbean island of Barbados: physical properties and origin, Atmos. Chem. Phys., 16, 14107–14130, https://doi.org/10.5194/acp-16-14107-2016, 2016.

Wu, H., Taylor, J. W., Langridge, J. M., Yu, C., Allan, J. D., Szpek, K., Cotterell, M. I., Williams, P. I., Flynn, M., Barker, P., Fox, C., Allen, G., Lee, J., and Coe, H.: Rapid transformation of ambient absorbing aerosols from West African biomass burning, Atmos. Chem. Phys., 21, 9417–9440, https://doi.org/10.5194/acp-21-9417-2021, 2021.

Yu, H., Tan, Q., Chin, M., Remer, L. A., Kahn, R. A., Bian, H., Kim, D., Zhang, Z., Yuan, T., Omar, A. H., Winker, D. M., Levy, R., Kalashnikova, O., Crepeau, L., Capelle, V., and Chedin, A.: Estimates of African Dust Deposition Along the Trans-Atlantic Transit Using the Decade-long Record of Aerosol Measurements from CALIOP, MODIS, MISR, and IASI, J. Geophys. Res.-Atmos., 124, 7975–7996, https://doi.org/10.1029/2019JD030574, 2019.

Zauscher, M. D., Wang, Y., Moore, M. J. K., Gaston, C. J., and Prather, K. A.: Air Quality Impact and Physicochemical Aging of Biomass Burning Aerosols during the 2007 San Diego Wildfires, Environ. Sci. Technol., 47, 7633–7643, https://doi.org/10.1021/es4004137, 2013. Zhang, R., Khalizov, A. F., Pagels, J., Zhang, D., Xue, H., and McMurry, P. H.: Variability in morphology, hygroscopicity, and optical properties of soot aerosols during atmospheric processing, P. Natl. Acad. Sci. USA, 105, 10291–10296, https://doi.org/10.1073/pnas.0804860105, 2008.

Zuidema, P., Xue, H., and Feingold, G.: Shortwave Radiative Impacts from Aerosol Effects on Marine Shallow Cumuli, J. Atmos. Sci., 65, 1979–1990, https://doi.org/10.1175/2007JAS2447.1, 2008.

Zuidema, P., Sedlacek III, A. J., Flynn, C., Springston, S., Delgadillo, R., Zhang, J., Aiken, A. C., Koontz, A., and Muradyan, P.: The Ascension Island Boundary Layer in the Remote Southeast Atlantic is Often Smoky, Geophys. Res. Lett., 45, 4456–4465, https://doi.org/10.1002/2017GL076926, 2018.

Zuidema, P., Alvarez, C., Kramer, S. J., Custals, L., Izaguirre, M., Sealy, P., Prospero, J. M., and Blades, E.: Is Summer African Dust Arriving Earlier to Barbados? The Updated Long-Term In Situ Dust Mass Concentration Time Series from Ragged Point, Barbados, and Miami, Florida, B. Am. Meteorol. Soc., 100, 1981–1986, https://doi.org/10.1175/BAMS-D-18-0083.1, 2019.